

THESIS FOR THE DEGREE OF DOCTOR OF PHILOSOPHY

Marine Propeller Optimisation - Strategy and Algorithm Development

FLORIAN VESTING



Department of Shipping and Marine Technology

CHALMERS UNIVERSITY OF TECHNOLOGY

Gothenburg, Sweden
2015

Marine Propeller Optimisation - Strategy and Algorithm Development

FLORIAN VESTING

ISBN 978-91-7597-263-3

© FLORIAN VESTING, 2015

Doktorsavhandlingar vid Chalmers tekniska högskola

Ny serie nr. 2015:3944

ISSN 0346-718X

Department of Shipping and Marine Technology

Division of Marine Technology

Chalmers University of Technology

SE-412 96 Gothenburg

Sweden

Telephone: +46 (0)31-772 1000

Cover:

Marine propeller manufacturing ©Rolls-Royce Plc. Reproduced with permission.

Printed by Chalmers Reproservice

Gothenburg, Sweden 2015

Marine Propeller Optimisation - Strategy and Algorithm Development
Thesis for the degree of Doctor of Philosophy
FLORIAN VESTING
Department of Shipping and Marine Technology
Division of Marine Technology
Chalmers University of Technology

Abstract

Recent trends in the shipping industry, e.g., expanded routing in ecologically sensitive areas and emission regulations, have sharpened the perception of efficient propeller designs. Currently, propeller efficiency, estimated fuel consumption and, more often, propeller-radiated noise are parameters that steer the business Zeitgeist. However, a practical propeller design that performs reliably and sufficiently throughout the lifetime of a ship requires numerous limitations, which are typically in conflict with the objectives. This requires judgement by experienced propeller designers to make decisions during the design process. To be ahead of competitors, a propeller designer needs to present a better design for a specific purpose, in a shorter time and at lower costs than the adversary. The current challenge for propeller designers is to develop a propeller that fulfils all the requirements and expectations within a short time frame.

The increasing interest in designing the optimal propeller shape is the motivation for this thesis, whose purpose is to further improve the state-of-the-art of the propeller design procedure by means of supplementing the propeller designer with automated optimisation. The art of designing a propeller, with the multi-disciplinary evaluation and consideration of numerous limitations, yields a systematic investigation of the design space, which is due to the generally limited time. Automated optimisation can fill the design space with numerous designs that gravitate, guided by the optimisation algorithm, towards an optimal design. This thesis therefore examines two tracks: i) the development of strategies and concepts for propeller optimisation, with the objective of developing optimisation algorithms that enhance the convergence and consideration of constraints, and ii) the extension and exploration of constraints that are adapted to the principles and design considerations of a typical manual design procedure.

Throughout this thesis, automated propeller design is improved. Population-based optimisation algorithms, design strategies and constraints, which automatically judge the cavitation on the propeller, are further developed. Additional constraints and limitations are added to the optimisation procedure, which are often neglected in study cases but which commonly have to be considered by designers. The algorithms and constraints are implemented in the designer's toolbox for computer-aided propeller design and can be used on an everyday design task with access to all the analysis tools available to the designer.

Keywords: constrained optimisation, marine propeller, cavitation, genetic algorithm, PSO, Kriging, artificial neural network, RANS, potential flow

To my father.

Preface

This thesis presents the work performed in the Hydrodynamics Group of the Department of Shipping and Marine Technology, Chalmers University of Technology, during 2010 to 2015. This PhD project was supported by the Department of Shipping and Marine Technology and by Rolls Royce through the University Technology Centre in Computational Hydrodynamics.

Many people helped me in completing this PhD project. It is an unfair task to acknowledge all the people who made this PhD thesis possible with a few words. But I will do my best. I want to sincerely thank my supervisor Professor Rickard Bensow for his constant encouragement, dedicated time and many discussions that we had. I have been amazingly fortunate to have an advisor who gave me the freedom to explore on my own, and at the same time the guidance to recover when my steps faltered. I would also like to thank Professor Lars Larsson, who a great part in setting up the project, and Kai-Jia Han for her comprehensive preceding work on numerical propeller optimisation.

With great appreciation, I am very grateful to Rikard Johansson, Göran Grunditz and Johan Lundberg at Rolls Royce AB for their support, sharp insights and enthusiasm for propeller design. Thank you very much for so many good discussions, inputs and for appreciating my research. Thank you Robert Fransson; working together with you was always great fun!

My dear colleagues at the Department of Shipping and Marine Technology have without exception been inspiring and provided a great working environment. Thank you very much Luis, Arash, Jonas, Francesco, Nicole, Lotta, Hiba, Elma, Andreas, Johannes, Claes, ... and many more.

I am deeply grateful to my parents for their faith in me and for allowing me to be as ambitious as I wanted.

At last I do not know how to begin with saying thank you to my soul mate, my best friend and my beloved wife, Sabine. I would like to thank you for your support, sympathy and unconditional love; without you this would not have been possible. I thank my family - Sabine, Leia and Felix, you make life fun! I love you guys!

Gothenburg, September 2015
Florian Vesting

Contents

Abstract	i
Preface	v
Contents	vii
List of appended papers	ix
Nomenclature	xi
1 Introduction	1
1.1 Background	4
1.2 Motivation	5
1.3 Composition of this thesis	6
2 Propeller Design	9
2.1 Problem description	9
2.2 Preliminary design	12
2.3 Design analysis and optimisation	14
2.4 Design evaluation	15
3 Numerical Methods	17
3.1 Potential flow propeller analysis model	17
3.2 Prediction of propeller cavitation	20
3.3 Unsteady propeller forces	21
3.4 Propeller-induced pressure pulse	22
3.5 Hybrid-RANS flow simulation	23
4 Optimisation	29

4.1	Deterministic methods	29
4.2	Non-deterministic methods	32
4.3	Meta-models	36
5	Summary of the work in the appended papers	39
5.1	Paper I	39
5.2	Paper II	40
5.3	Paper III	42
5.4	Paper IV	43
5.5	Paper V	44
5.6	Paper VI	46
6	Discussion	49
7	Conclusion	55
8	Further Work	57
	References	59

List of appended papers

This thesis consists of an extended summary and the following appended papers:

- Paper I** F. Vesting and R. Bensow (2011). “Propeller Optimisation Considering Sheet Cavitation and Hull Interaction”. *Proceedings of the Second International Symposium on Marine Propulsors*. (Hamburg, Germany). Ed. by M. Abdel-Maksoud. Hamburg University of Technology, 79–88
- Paper II** F. Vesting and R. E. Bensow (2014). On surrogate methods in propeller optimisation. *Ocean Engineering* **88.0**, 214–227
- Paper III** F. Vesting, R. Johansson, and R. Bensow (2013). “Parameter Influence Analysis in Propeller Optimisation”. *Proceedings of the Third International Symposium on Marine Propulsors*. (Launceston, Tasmania, Australia). Ed. by J. Binns, R. Brown, and N. Bose. University of Tasmania, 397–404
- Paper IV** F. Vesting and R. Bensow. Particle Swarm Optimisation: An Alternative in Marine Propeller Optimisation? Manuscript submitted for publication to OPTE Journal of Optimization and Engineering
- Paper V** F. Vesting, R. Gustafsson, and R. Bensow. Development and Application of Optimisation Algorithms for Propeller design. Manuscript submitted for publication to STR Journal of Ship Technology Research
- Paper VI** F. Vesting, N. Costa, R. Johansson, R. Gustafsson, and R. Bensow. Procedure for application-oriented Optimisation of Marine Propellers. Manuscript to be submitted for publication to OE Journal of Ocean Engineering

Contributions to the papers:

The author of this thesis contributed to the ideas presented, was responsible for the planning of the paper, performed the numerical computations and wrote the manuscripts.

Nomenclature

Acronyms

<i>AS</i>	Adaptive Surrogate-assisted
<i>BEM</i>	Boundary Element Method
<i>CCNN</i>	Cascade Correlation Neural Network
<i>CPP</i>	Controllable Pitch Propeller
<i>CSR</i>	Continuous Service Rating equivalent to NCR
<i>CVM</i>	Constraint Violation Measure
<i>DNV</i>	Det Norske Veritas
<i>EASM</i>	Explicit Algebraic Stress Model
<i>FAST</i>	Fourier Amplitude Sensitivity Test
<i>FFNN</i>	Feed Forward Neural Network
<i>FPP</i>	Fixed Pitch Propeller
<i>IMO</i>	International Maritime Organisation
<i>ITTC</i>	International Towing Tank Conference
<i>LES</i>	Large Eddy Simulation
<i>L_{pp}</i>	Length between perpendiculars
<i>MARIN</i>	Maritime Research Institute Netherlands
<i>MCR</i>	Maximum Continuous Rating
<i>NCR</i>	Maximum Continuous Rating equivalent to CSR
<i>RANS</i>	Reynolds Averaged Navier-Stokes
<i>SANA</i>	Surrogate Assisted Neighbourhood Assessment
<i>SMCR</i>	Specified Maximum Continuous Rating
<i>VLM</i>	Vortex Lattice Method

Variables and notations

(u, v, w)	Velocity components in (x, y, z) directions
(x, y, z)	3D Cartesian coordinates
η, η_B	Propeller efficiency behind ship
η_H	Hull efficiency
η_S	Shaft efficiency
Γ	Discrete vortex
$\gamma(x)$	Vorticity distribution on 2D
Γ_B	Strength of bound vortex on blade surfaces
Γ_W	Strength of free shed vortex on wake surfaces
\mathbf{n}	Normal vector to camber surface
\mathbf{v}	Velocity vector
ω	Dissipation rate
ϕ	Position angle for wake velocity
ϕ	Velocity potential
ρ	Fluid mass density
θ	Blade angle

θ_0	Angular coordinate
A_n, B_n	Fourier series harmonic coefficients
D	Propeller diameter
g	Acceleration due to gravity
h	Cavity thickness
J_S	Advance ratio
k	Turbulence kinetic energy
K_Q	Propeller torque coefficient
K_T	Thrust coefficient
L	Lift
l	Cavity length
n	Harmonic number
n	Number of propeller revolutions per second
p	Pressure
p	Propeller induced pressure pulses
P_B	Brake power
$q(x)$	Cavity source distribution
Q_B	Discrete line sources for blade thickness
Q_C	Discrete line sources for cavity thickness
R	Propeller radius
t	Time
U_∞	Flow speed at infinity
V_a, V_r, V_t	Time-averaged velocity
V_S	Ship speed
w_t	Total wake fraction
y^+	Non-dimensional wall distance
Z	Number of propeller blades

Any sufficiently advanced technology is indistinguishable from magic.

Arthur C. Clarke

1 Introduction

The marine screw propeller is a fascinating invention. It transmits power into a fluid medium by converting rotational motion into thrust. Hydrofoils are arranged on a shaft, which are shaped and aligned such that a pressure difference develops between both blade sides, thereby accelerating the fluid. Today's propeller blade shapes are highly complex free-form surfaces that require careful design considerations and accurate manufacturing engineering.

Inspired by the Archimedes' screw and Leonardo da Vinci's principle of a helicopter, the first concepts of ship propellers emerged in the 18th century as suggestions to propel ships, e.g., those by *Robert Hooke*, *Daniel Bernoulli* and *James Watt*. These earlier fan-like propellers resemble today's propellers in appearance. However, the first marine propellers used in applications were Archimedean screw-type propellers, which powered a submarine developed by *David Bushnell*. The developments accelerated at the beginning of the 19th century, when the increased power and reliability of steam engines required an improvement in propulsion for sea-going ships. Several inventors equipped steam-driven ships with different types and constellations of propellers. *Josef Ressel*, for instance, designed an Archimedean screw-type propeller with two blades, each of a single revolution, and equipped the steam vessel 'Civetta' with this propeller in 1829. Figure 1.1 provides the handwriting of Josef Ressel for his marine propeller.

In 1836, *John Ericsson* proposed a propulsion system of two contra-rotating propellers based on the Bernoulli-type propeller. The propellers were mounted behind the rudder, which resulted in hindered manoeuvrability. *Francis Pettit Smith* tested a wooden Archimedean screw, designed with two turns, on a 30-foot vessel in 1837. The propeller accidentally broke, and suddenly, with only a single turn left, the achievable ship speed doubled. These inventors, to name only a few, contributed to the development of the propeller. All of them encountered suspicion and initial opposition from stakeholders at the time. The fact that propeller design stabilised only towards the end of that century highlights that the effectiveness of the propeller was not entirely understood. However, screw propellers were beneficial in multiple fields, compared to typical paddle propulsion, and became the dominant propulsion type. Since then, many attempts have been made to minimise the amount of input energy to the propeller; however, the general form evolved in the 19th century.

Propellers are still under development, and their appearance today differs from that of propellers from two or three decades ago. At present, modifications to the propeller design are widely motivated by technology developments (e.g., manufacturing technology or material technology), regulations (e.g., DNV SILENT class notation (DNV, 2010)) or costs (e.g., production and operation costs), which are driven by the general developments of shipping. The globalised

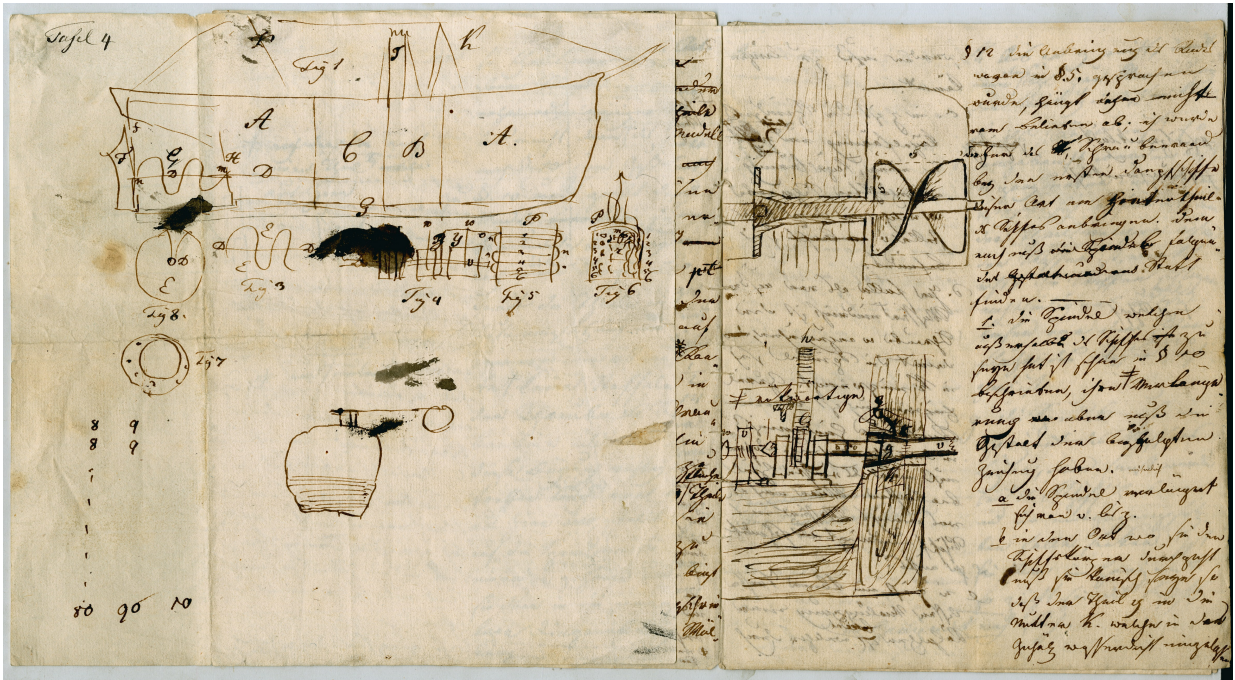


Figure 1.1: Handwriting of Joseph Ressel (drawing of a marine propeller and section of the ship hull); undated - from the TMW-Archiv, BPA10915/17

business world yielded an increased need for transportation, which implicitly, due to the cost advantage of size (economies of scale), resulted in an increase in ship size. During the second half of the last century, the commercial fleet approximately tripled in number of ships, while the gross tonnage increased by a factor of more than six (in the world's shipping fleet for ships of 100 gross tones and more) (Hildebrand, 2009). Consequently, the installed power in the ships increased and propellers needed to transfer more energy to the water; the cavitation phenomenon arose more frequently on the propeller. Cavitation has to be considered and controlled by the propeller designer, and it has certainly changed how the propeller blade shape has evolved. In the future, new materials such as composites or regulations on radiated noise might initiate further changes to the way in which we design propeller blades.

For a long time period, the order of a propeller has been considered as a question of investment costs. However, with expanded routing in ecologically sensitive areas, awareness of the propeller-radiated noise level and environmental concerns have arisen. Together with the increasing bunker prices of recent years, expected average emission growth of 95% by 2050 (Smith et al., 2014), and emission regulations, these trends have sharpened the perception of efficient propeller designs and have affected the way in which propellers are ordered. Consequently, the focus of propeller design shifted again, and propeller efficiency (η_B) became an important design criterion. The propeller efficiency directly impacts the required power output of the engine (P_B)

$$P_B = \frac{R_T V_S}{\eta_H \eta_B \eta_S} \quad (1.1)$$

and thus the fuel consumption of the engine with the specific fuel consumption sfc

$$\dot{m}_f = P_B sfc. \quad (1.2)$$

Although efficiency is a qualified measure for the extent of how well an input is used to achieve the desired output, it alone is not sufficient for propeller design tasks. However, suppliers have

experienced a change in the customers' perspective towards a situation in which only the propeller efficiency and fuel consumption have become the major selection criteria (Grunditz, 2015).

The additional awareness enhances competition. In fact, suppliers more frequently attend comparative performance competitions, where the ranking is based entirely on the propeller efficiency and estimated fuel consumption. In such competitions, the fuel consumption is commonly verified in impartial test facilities, where model tests are conducted with a self-propelled model and the results are converted to full scale according to the standard ITTC method (ITTC, 1999). This competition and evaluation practice is generally improving the propeller design, yet it has initiated a worrying trend of sub-optimal designs with high-efficiency performance, disregarding other performance characteristics, e.g., risk for erosion, propeller-induced vibration and variable operating conditions (Grunditz, 2015).

Propeller design is a highly complex procedure, involving many influencing factors. Tuning the propeller geometry towards efficiency also changes its characteristics with regard to vibration, inboard noise and cavitation behaviour, which will most likely occur when the propeller is in operation. The propeller experiences varying inflow conditions while travelling through the circumferential wake. This causes a varying load on the propeller blade during one revolution and results in a local pressure drop around the blade. Depending on the operating conditions, e.g., submergence of the propeller shaft or rotational speed, the pressure sags below the vapour pressure and cavitation, i.e., vapour pockets in the liquid, can be observed at the propeller. When again entering high-pressure regions, the cavities collapse extremely rapidly and may cause noise and vibration, which are transferred to the ship's hull, and cause erosion on the propeller or the rudder. Cavitation and propeller-induced pressure pulses are the most evident propeller effects contradictory to efficiency. Consequently, the only solution is to find a trade-off blade geometry that is adapted to the flow and therefore only valid for a certain ship and the specific operating conditions. To satisfy the ship owner's expectations and to deliver a practical design, the designer has to not only consider and control the cavitation but also constrain static and dynamic blade stresses, classification requirements and, in the case of controllable pitch propellers, hub strength and blade clearance.

Thus, propeller design is truly an art of trading performances and requirements, which is naturally a multi-objective and multi-disciplinary procedure and which can only be accomplished in an iterative manner. Common practice is to develop a preliminary design concept and improve this by subsequently evaluating all applied objectives and constraints to find the best compromise. The various requirements together with seemingly countless modifications to such a free-form surface lead to a large number of alternatives to be studied and thus place restrictions on the numerical analysis tools. The blade geometry is, during the design synthesis, evolved by the designer's experience towards the design philosophy and considered as the optimal design. With sufficient time, a designer can efficiently analyse the design space and reach, driven by the knowledge, the best possible design. In such a procedure, time is the most limiting restriction.

The length of time available for a product being conceived until it is ready for sale is one of the most important factors in a world that is changing rapidly at an accelerating pace. This holds for most of the engineering design tasks and in particular for the propeller design because each is a unique layout for a certain ship. To be ahead of competitors, a propeller designer needs to present a better design for a specific purpose in a shorter time and at lower costs than the adversary. The current challenge for propeller designers is to develop a propeller that fulfils all requirements and expectations within the short time length available in the competition races.

Thus, although the evaluation of propeller performance requires highly unsteady and physically profoundly complex simulations, it is common practice to apply less accurate but faster potential methods (e.g., Mishima, 1996; Griffin et al., 1998; Han et al., 2006; Gaggero et al., 2009; Lee et al., 2010; Bertetta et al., 2012). In an early design stage, potential methods are indispensable and are, in a later design stage, commonly accompanied by either experiments of model propellers or high-fidelity numerical simulations, or both, to validate the performance prediction.

1.1 Background

There have been several different approaches to improve propeller design within the past three decades. Burnside et al. (1979) presented, for instance, one of the first propeller design recommendations with special considerations regarding propeller-induced vibrations. Both analytical and experimental techniques were considered and indicated that cavitation has a significant influence on the hull pressure.

More recently, (Mishima, 1996) presented the optimisation of propeller blade geometry with respect to sheet cavitation, which was predicted using a vortex lattice method (VLM). Mishima (1996) minimised the torque in a single-objective approach, where the objective function was approximated first by a linear and finally by a quadratic function. The function coefficients were determined using a numerical propeller analysis program. Hence, the actual optimisation was accomplished by employing a classical optimisation method of linear and quadratic programming.

Griffin et al. (1998) further developed the non-linear optimisation method and included a quadratic skew distribution. The propeller performance was again analysed using a VLM with cavitation prediction. Griffin et al. (1998) applied constraints on the minimum blade pressure distribution and thereby prevented the onset of bubble cavitation. The optimisation yielded, with further applied constraints on the cavity area and maximal cavity volume, an improved propeller design.

Automated propeller optimisation has emerged more frequently in recent years for accomplishing a large number of design alternatives and thereby supporting the designer during the design synthesis and reducing design lead time. Foeth (2015) presented a propeller geometry parametrisation based on database records and the multi-objective optimisation in the behind condition, applying the derived parameters. Thus, the optimisation was performed with full interaction between the propeller changes and hull changes. However, this was computationally intensive, and no constraints were considered. It is hypothesised that a preliminary optimisation is performed to determine the main parameter ranges. Berger et al. (2014) presented such an idea in a two-stage optimisation with propeller hull interaction applied in the second stage, after evaluation of a multi-objective optimisation in a given wake condition. This is an efficient intermediate step for assisting the designer in finding the optimal design for a given hull geometry. However, in the presented approach, only a constraint on thrust equality was applied, and the objective function was related to the applied weight factor.

Constrained propeller optimisation was, e.g., presented by Han et al. (2006) with a weighted multi-objective propeller blade optimisation in a given wake and with constraints on sheet cavitation. The results align with Griffin et al. (1998), showing considerable improvements in cavitation performance when applying cavity volume and area constraints.

Similarly, Kamarlouei et al. (2014) applied an optimisation in a fixed wake, with cavitation

constraints on the blade loading (Keller criteria) and the Bucket criteria. In contrast to Han et al. (2006), Kamarlouei et al. (2014) also included constraints for the blade strength, although with simplification to cantilever beam theory. Bertetta et al. (2012) presented the multi-objective optimisation of a controllable pitch propeller (CPP), with the main aim of reducing the face cavitation and thereby the resulting radiated noise. The common dominator of the aforementioned examples is the applied numerical evaluation of the propeller performance, which is based on potential methods. However, the applied cavitation constraints are based on general characteristics, e.g., the maximum cavitation volume or the cavity areas, and constraints on blade strength were only included by Kamarlouei et al. (2014).

1.2 Motivation

The recent work outlined above highlights the growing interest in designing the optimal propeller shape. However, in practice, evaluations of numerous limitations and parameters require various judgements by experienced propeller designers to make decisions during the development, where lead time is the most limiting factor during the investigation of design alternatives. With the enhanced accuracy of numerical tools and increasing computational power, particularly in desktop workstations, this task can be facilitated by automated optimisation. The challenge is to develop algorithms that not only create variants automatically but that also handle constraints and make decisions in favour of the designer's decision to find the global optimum.

The purpose of this thesis is to further improve the state-of-the-art of the propeller design procedure by supplementing the propeller designer with automated optimisation. The overarching research question is therefore the following:

How can optimisation be adapted to propeller design on an everyday use basis to efficiently assist the designer using automated optimisation and simultaneously enhance the multi-disciplinary evaluation of the manual design procedure to reduce the lead time in product development?

This thesis therefore examines two tracks: i) the development of strategies and concepts for propeller optimisation, with the objective of developing optimisation algorithms that enhance convergence and consideration of constraints, and ii) the extension and exploration of constraints that are adapted to the principles and design considerations of the manual design procedure. The art of designing a propeller, with the multi-disciplinary evaluation and consideration of numerous limitations, limits a systematic investigation of the design space, which is due to the available time generally being limited. With automated optimisation, we can fill the design space with numerous designs, which gravitate, guided by the optimisation algorithm, towards an optimal design. Figure 1.2 exemplifies the distribution of variants on objective space through the manual approach (●), where the designer creates several (typically 10-30) designs and determines the most suitable among these. However, with automatically generated designs (●) that incorporate the design constraints and strategies, the design space can readily be filled to find better design alternatives faster.

An automated propeller optimisation procedure requires a judgement of a design variant without interaction of the designer. The objective of this thesis is thus to develop constraints that condense information of the design into single values while enabling connection to geometry changes to the critical design characteristics. To achieve this objective, this thesis focuses in particular on constraints in cavitation that adapt to the shape of the cavity. The work on cavitation constraints is initiated in paper I and is continuously developed further and finalised in paper V. However,

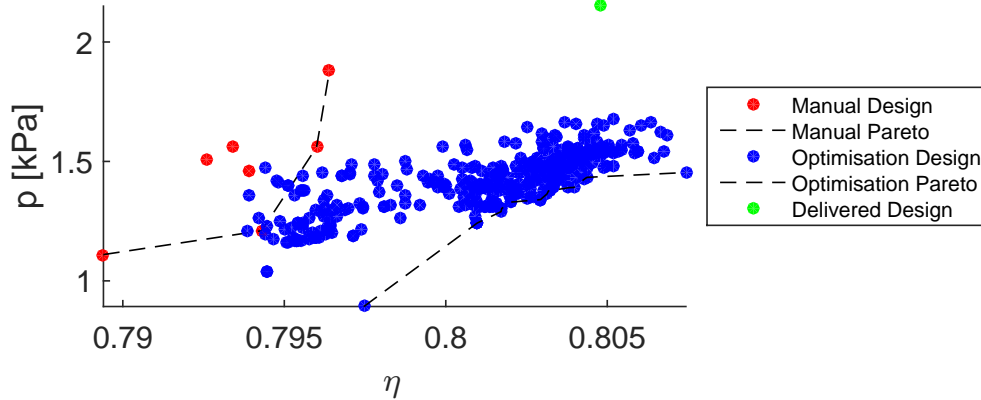


Figure 1.2: Design space for manually generated solutions and solutions from an automated optimisation; real life example of the manual design procedure and subsequently conducted optimisation.

because the propeller design is a compromise of several constraints, an algorithm is required that particularly considers constraints together with a constraint-handling technique that resembles the decisions of an experienced designer. To reduce the lead time, the goal of this thesis is also to evaluate and apply meta-models during an optimisation that can fill the design space more quickly with computationally inexpensive evaluations and thereby increase the convergence of the algorithm. The evaluation of meta-models is included in the work in paper II, the development of the algorithms is presented in papers IV and V, and the review of the proposed algorithms and strategies is presented in paper VI.

1.3 Composition of this thesis

This thesis is conducted within the Rolls-Royce University Technology Center (UTC). It is composed of six studies, which are interconnected through the two main tracks: the development of optimisation strategies and propeller design constraints. Investigated designs are chosen from the Rolls-Royce design database for the representation of contemporary propeller designs and possible comparison with delivered benchmarks. Figure 1.3 outlines the progression of the work performed and the gained knowledge throughout this thesis.

The first paper (paper I) is a continuation of the work performed by Han et al. (2006) and Han (2008), where in both cases the propeller geometry is optimised, but one in a fixed wake (Han et al., 2006) considering cavitation and one together with a coupled a Reynolds-Averaged Navier-Stokes (RANS) solver and a propeller analysis code, without cavitation consideration (Han, 2008). In paper I, we therefore consider both optimisation in the behind condition and examination of cavitation constraints. Papers II and III are closely related to the first paper and are intended to answer the question that emerged in paper I: *How can we improve the convergence of the optimisation algorithm?*

In papers IV and V, the optimisation algorithms are refined, and an adaptive surrogate-assisted algorithm and a new neighbourhood assessment algorithm are introduced in paper V together with the outline of optimisation strategies and new cavity shape constraints. Paper IV introduces an optimisation assessment and optimisation quality ascertainment strategy. These developments form the platform for paper VI, in which the strategies and algorithms are tested on seven test propellers. The results of the different optimisation cases are compared among each other and with a corresponding benchmark design, manually designed and delivered by Rolls-Royce AB. From

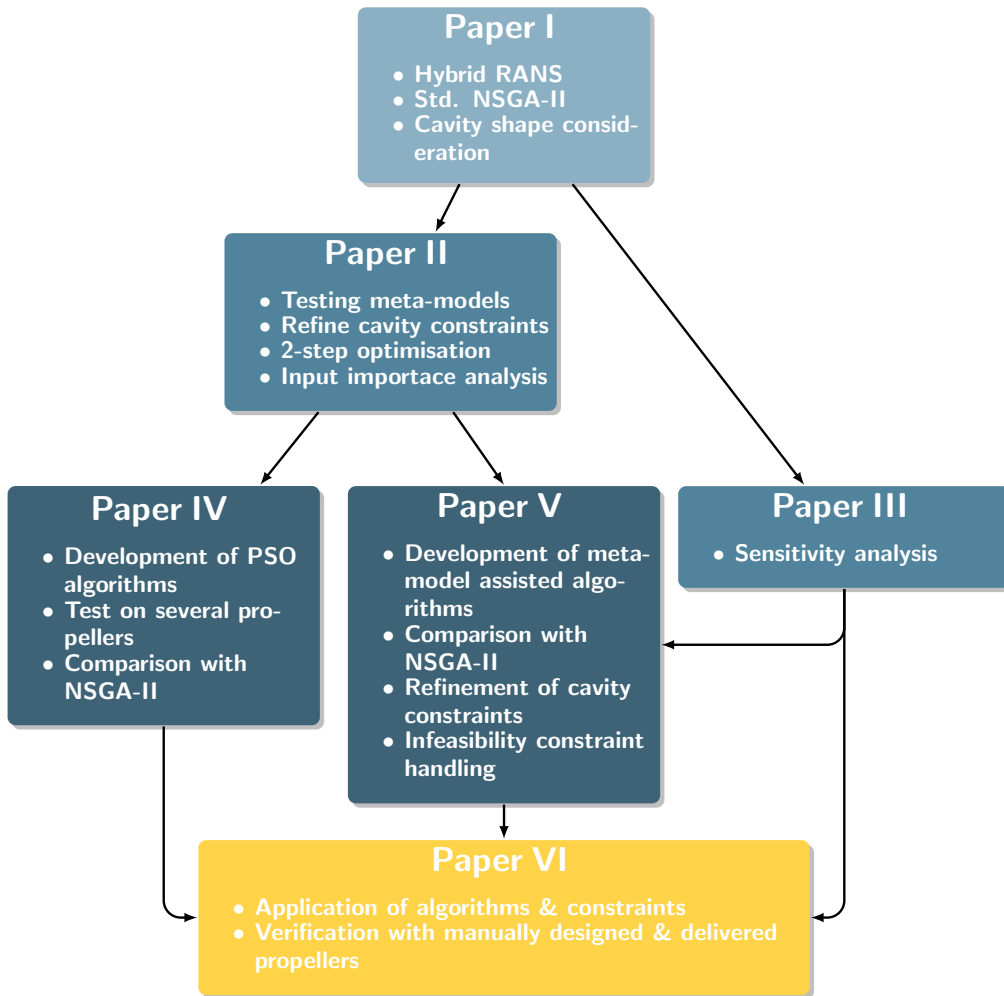


Figure 1.3: Informational illustration of the work performed and connection of the research

the test set-up and the evaluations, we propose a two-stage optimisation procedure for marine propeller design.

Chapter 2 provides an introduction to the propeller design procedure and identifies the operation range delimitations of the optimisations. Chapter 3 contains a brief summary of the applied numerical methods, as well as additional considerations regarding the computational set-up used in paper I. Optimisation is discussed in Chapter 4 together with the development of the optimisation framework.

The computer is incredibly fast, accurate, and stupid. Man is unbelievably slow, inaccurate, and brilliant. The marriage of the two is a force beyond calculation.

Leo Cherne

2 Propeller Design

Propeller design is the art of synthesising multi-disciplinary requirements and limitations into a cohesive final product that efficiently meets the features of a specific ship. It is an iterative procedure that can generally be divided into three interacting phases: i) the problem description, ii) the preliminary design and iii) the design analysis and optimisation phases. A flowchart of the propeller design phases is presented in figure 2.3, which provides an overview of the three phases and includes both tools that the designer uses and the expected outcome of each phase. In common engineering design problems, there is a fourth phases in which the design is evaluated, commonly with a prototype. However, this is rarely possible in propeller design due to the uniqueness of the designed propeller and because the evaluation occurs using full-scale sea trial tests with the final product. Therefore, propeller design requires particular attention in the design analysis and optimisation phase. Automated optimisation approaches can support the designer in finding better designs faster.

2.1 Problem description

The primary task in the problem definition phase is the determination and correct selection of the design point for the propeller. However, this requires the determination of the propeller type and the selection of an engine. Hence, the problem description phase typically starts with an evaluation of the vessel: What is the ship's purpose? Where will it operate? What is the hull maintenance procedure? Various operating conditions that the ship experiences during its lifetime are usually summarised in a mission profile of the ship, which is provided by the ship's owner. It determines the portion of time that a ship travels at a certain speed and thus outlines the economical design point. However, the propeller also has to match the engine characteristics for a good performance. The wrong selection of the design point results in suboptimal operation of the engine at other operating conditions. This is particularly important for a fixed pitch propeller (FPP) because the design is only valid for one condition, but even the sectional profiles of controllable pitch propellers (CPP) are optimised for only one inflow condition.

The ship's requirements also determine the propulsor or rather the propeller type. Systematic series data, e.g., by Van Manen (1966), Blount (1993) or Tachmindji et al. (1957), assist the designer in selecting a suitable propeller type. However, initial costs, running costs and maintenance costs also determine the type of propeller. Once the propeller type and the engine are selected, the propeller demand and engine power supply need to be matched, considering that the ship

and the propeller will be subjected to fouling, different weather conditions and different loading conditions. In figure 2.1a a typical, yet simplified, situation of a propeller demand curve matched to the engine characteristics is given for the correct propeller design point at the engine's MCR. A failure in the pitch selection of the propeller pitch will lead to an over-pitched or under-pitched design. Both cases prevent achieving the maximum engine power; either the torque limit will hinder the engine from developing its maximal power in the case of an over-pitched propeller or the engine speed limit will diminish the maximum available power.

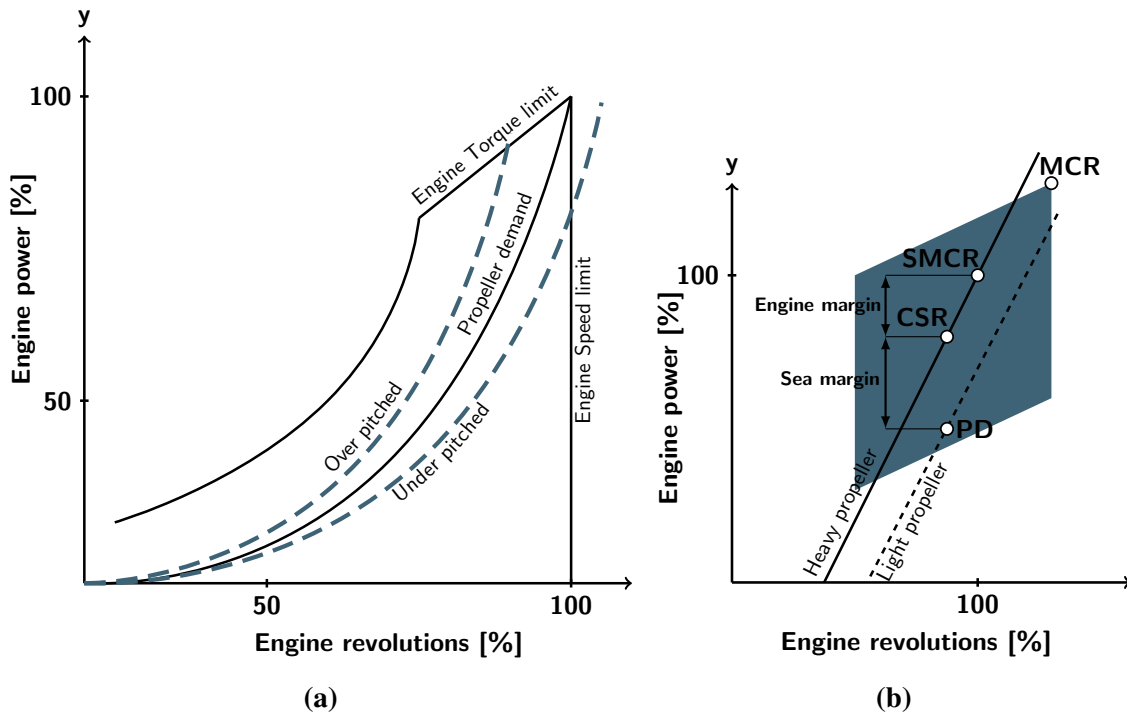


Figure 2.1: Determination of propeller design point; (a) typical engine characteristics and propeller demand curve, (b) propeller design point and engine layout

Consequently, margins have to be considered for the service conditions of the ship, e.g., change in displacement, increased hull roughness due to age and fouling, and increase in propeller roughness and wind and waves, commonly referred to as sea margin.

Sea Margin In practice, this does not mean that the ship must meet full speed in all weather conditions, but rather, that it can sustain its service (design) speed over a realistic percentage of conditions (ITTC, 2008).

Hence, the propeller designer considers two propeller demand curves: a light propeller curve for a clean hull and calm weather conditions and a heavy propeller curve for an aged hull and heavy weather condition.

The propeller design point is typically placed on the light running curve as a combination of desired ship speed (from the mission profile) and the required power. The propeller design point is either given power consumption with or without accounting for the sea margin. In figure 2.1b, the design point is defined on the light propeller curve. The continuous service point is obtained at the same engine speed, but with a sea margin of typically 10-15% of the design point's power demand. The continuous service propulsion point, also referred to as continuous service rating (CSR) or normal continuous rating (NCR), is provided on the heavy propeller curve and is valid for a fouled hull under heavy weather conditions. An additional margin (engine margin) is often introduced to

reduce maintenance costs in keeping the machine away from peak performance over the lifetime.

Engine Margin *The engine operation margin describes the mechanical and the thermodynamic power reserve for the economical operation of the engine(s) with respect to reasonably low fuel and maintenance costs (ITTC, 2008).*

The final margin yields the specified MCR (SMCR), which is the maximum rating required for continuous operation of the engine. The SMCR may be different from the engine nominal maximum continuous rating (MCR), which is the engine’s limit for continuous operation (nominal MCR in figure 2.1b).

The shaded area in figure 2.1b presents the engine layout diagram, limited by two constant engine speed lines and two constant mean effective pressure lines. Within the outlined area, the SMCR point can be defined to meet the optimum operation profile for the ship, where the lowest fuel consumption will be achieved at 70 to 80% power of SMCR for both electronically and mechanically controlled engines (MAN, 2011).

Once the engine and propulsion points are defined, the engine load diagram for the main engine can be drawn, e.g., figure 2.2, which defines continuous and overload limits for the engine. For an FPP without a shaft generator, the continuous service operation is limited by the lines of the engine’s torque and speed limit in figure 2.2. The maximum speed limit of an engine is typically defined as 105% of SMCR, and the torque limit line provides the maximum combination of torque and speed. Thus, between the light propeller curve and the torque limit, there must be a sufficient margin considered when defining the design points. The propeller curve is given according to the propeller law, which is a cubic function, but these diagrams typically use logarithmic scales; thus, the curves are given as linear curves. The maximum engine speed limit may be extended to 105% of the engine’s nominal speed limit (extended speed limit) for a limited time span, e.g., to achieve the SMCR power during a sea tail with the light propeller curve.

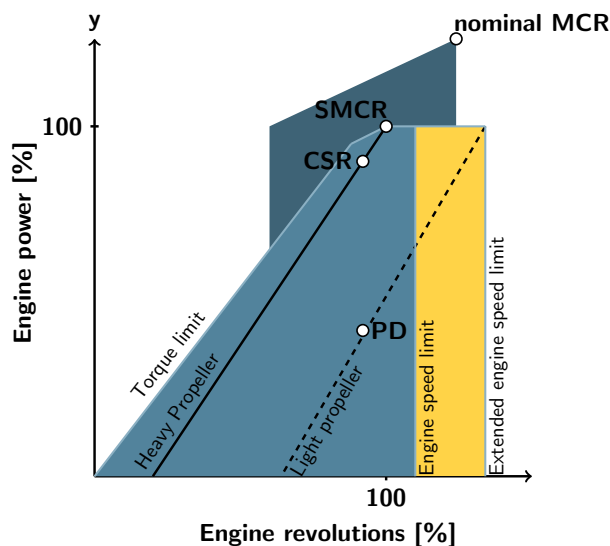


Figure 2.2: Standard engine load diagram for an FPP without shaft generator

2.2 Preliminary design

The basic design of the propeller is developed in the second design phase. In this phase, the designer determines the propeller diameter, blade area ratio (EAR), number of blades, pitch ratio and sectional shapes. In principle, two different methods aid the designer in this phase: development with the results of open-water tests of systematic series propellers and development based on circulation theory. The choice depends on the designer's philosophy and ability and on the frequency for needing to develop a propeller. Commercial suppliers typically base their preliminary designs on the second method: circulation theory.

When developing possible design alternatives, the designer considers the propeller diameter, which is typically limited by the hull shape but has the greatest impact on the propeller efficiency and the propeller-induced unsteady forces. A larger propeller diameter increases the propeller efficiency, but the hull efficiency abates, and a decreased distance from the propeller tip to the hull surface will increase the pressure pulses on the hull. The designer also needs to balance the diameter with consideration of the tip velocity, which increases with larger diameter (for a constant RPM) and thus increases the risk for tip vortex cavitation. In addition to the diameter, the number of blades also has a strong influence on the propeller efficiency, which is generally higher with less blades. However, more blades will reduce the unsteady propeller forces. The choice of the number of blades is limited by the type of propeller, e.g., a CPP typically limits the number to five blades, where the hub needs to accommodate the gear of each blade.

Once the fundamental geometry is determined, the designer can utilise a propeller series based on open-water experiments of a systematic series of propellers, varying design parameters such as the pitch ratio, blade area ratio or blade outline to determine the required ratios for the particular design case. The collected propeller performance data are then often integrated in regression equations to specify the propeller characteristics of a new propeller. Although propeller series are widely accepted and used, there is no wake adaptation, and the currentness of results is limited. For instance, the well-known propeller series MARINs B-Series propellers (Van Lammeren et al., 1969) is based on a parent model with a constant pitch distribution towards the tip and a low skew angle. Contemporary propeller designs, with a reduced tip loading and higher skew angles, achieve a similar level of pressure pulses as the B-Series propellers but with up to 3% higher efficiency. Optimisations of the preliminary propeller design based on propeller series are discussed, e.g., by Triantafyllou (1979) and Benini (2003).

The alternative to propellers series design is the application of circulation theory, e.g., lifting line theory (Lerbs, 1952), lifting surface theory by Greeley et al. (1982) or similar, with particular consideration of the blade tip geometry, as by Olsen (2001). Compared to the design with a propeller series, the required input is more demanding. The application of circulation theory already enables the adaptation to the ship's wake by optimising the circulation distribution in the radial direction to minimise the propeller torque for a required thrust. Consequently, the radial distribution of the circumferential average inflow, required thrust and profile section drag coefficients need to be known at that stage of the design. With such methods, the designer numerically creates a series of propellers to find the most suitable preliminary design as the starting point for the analysis and optimisation phase.

Methods based on circulation theory determine the optimal pitch and camber distribution for the given circumferential averaged inflow, where the optimal pitch distribution is calculated using a lifting line method. The camber distribution is subsequently calculated using a lifting surface

method, prescribing the obtained pitch and an initial camber distribution. The final camber is iteratively obtained by computing the fluid velocity on the surface and adjusting the surface until its normal component annuls (Kerwin et al., 2010).

How detailed the preliminary geometry can be elaborated in both cases, the propeller series and the application of circulation theory, depends on the representation of the geometry by each method. The capabilities of computer programs applying circulation theory may be different, but most of the codes are able to account for not only chord and blade thickness but also for skew and rake. Geometrical parameters, e.g., EAR, skew, rake and maximum thickness, can then be provided by the designer, usually given as non-dimensional distribution curves along the radius of the propeller. Such distribution curves are typically parameterised and can be controlled by a few parameters; their shapes represent the common design philosophy of the designer depending on the type of propeller and the ship type, size, break power and so forth. Foeth (2015), for instance, elaborate a parameterisation of the geometry distribution curves based on 1250 unique propellers in MARINs database.

In figure 2.3, the preliminary design and the design analysis and optimisation phases are connected to indicate that there is a possible iteration between the two design phases. The analysis and optimisation phase introduces restrictions, which are not considered in the preliminary design, and conflicts with the preliminary design may arise. The design process should be flexible enough to account for changes in the preliminary design.

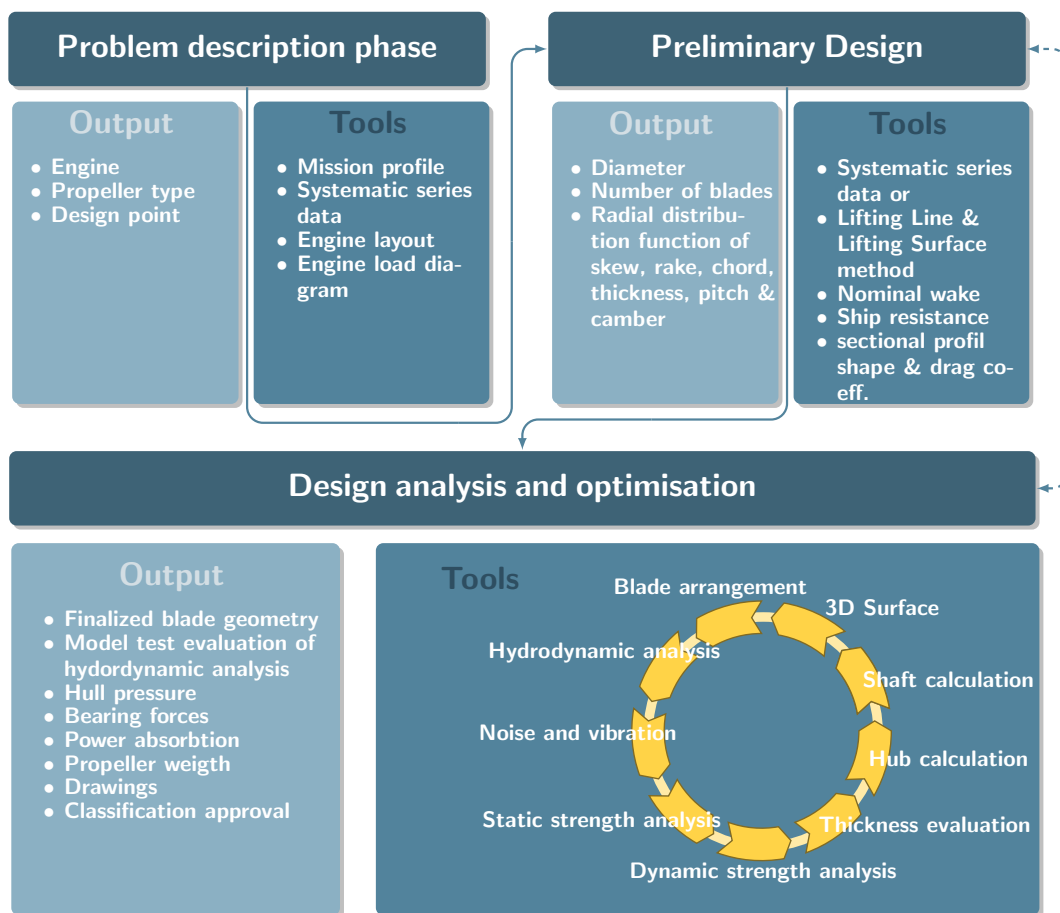


Figure 2.3: Design process of a propeller

2.3 Design analysis and optimisation

The preliminary design is elaborated in the design analysis and optimisation phase with numerical methods and experiments, respectively, to develop the detailed geometry. In this phase, the design is optimised with detailed changes of the blade geometry to find the best compromise. Unlike the preliminary design phase, where the blade geometry is only partly specified and partly *designed* using the numerical methods as an optimisation of circulation distribution, in the analysis phase, the entire geometry is known and the performance of the propeller is *analysed* using numerical methods. This analysis requires detailed inflow information, obtained either by simulation of the ship together with the propeller or by calculation of effective inflow velocities, for detailed estimation of the propeller forces and cavitation.

The design analysis and optimisation phase can also be accomplished by systematic series and empirical formulation. The application of numerical methods and model tests again depend on the capabilities of the designer and the requirements of the customer. For small vessels where only little information of the flow around the hull is known, the design procedure based on a series of propellers and an adaptation based on cavitation criteria, e.g. Keller criteria, propeller strength evaluation by cantilever beam theory followed by a fatigue estimate and blade thickness according to classification rules, may be sufficient. However, for larger vessels, propeller suppliers typically utilise numerical methods of variable fidelity and experiments of model propellers to evaluate the simulations.

The final part of the design phase finalises the design such that the propeller is ready for manufacturing. In addition to a detailed geometry representation, this also requires constraints that restrict the design and yield designs that are manufacturable and that conform with the classification rules. Hence, this phase is about manipulating the geometry iteratively to find the best compromise that is feasible and that provides the best performance. It is a design spiral that includes multi-disciplinary constraints and objectives and that is traversed by the designer several times. The process is presented as a continuous circle (figure 2.3); however, the cycle may be interrupted when the performance is not acceptable and design changes are required.

Typical constraints are cavitation, static and dynamic blade stresses and classification regulations that are often contradictory to the typical objectives (propeller efficiency, propeller-induced pressure pulse and blade weight). However, when the detailed geometry is already developed as a 3-dimensional surface, constraints apply on the arrangement of the blade on the hub, blade collision and details of the blade edges. The designer analyses the hydrodynamic performance to obtain the propeller forces and thus the power consumption and evaluates cavitation on the blade, which typically has to be constrained to reduce the risk for erosion. Propeller-induced vibration and noise are related to the hydrodynamic performance but often require specific calculations. Static strength and possibly ice loads acting on the propeller blades are, with contemporary blade shapes, calculated using finite element methods (FEM). The obtained maximum stress level is subsequently applied in a dynamic strength analysis to ensure the service life of the propeller. Classification approval requires not only providing a minimum blade thickness but also calculations of the hub and the shaft, e.g., blade bearing forces, blade bolt diameter or required oil pressure to pitch the blade in the case of a CPP.

The outlined iterative procedure requires an experienced propeller designer to systematically modify the geometry locally to accommodate all the requirements on the design. It can be come very time consuming to account for all multi-disciplinary evaluations. Therefore, an automated

optimisation can assist the designer in accomplishing this task faster and with a better quality of the final design.

2.4 Design evaluation

After the optimal propeller design is obtained, all limitations and demands are satisfied, and the design is approved, the propeller will be manufactured. The evaluation of the design is generally accomplished during full-scale speed and powering trials with the final product, which are typically conducted at the end of the ship-building phase with a new, light and clean hull. The problem of sea trials is to correct the measured data to ideal, typically contracted, conditions, which is addressed by ITTC (2002). It may also be required to evaluate the ship and propeller performance in service conditions to reduce operating costs and to collect data for possible sister ships (Andersen et al., 2005). Mismatching the specified design criteria results in costly modifications of the propeller.

3 Numerical Methods

There is a broad range of numerical simulation methodologies and tools that can be consulted for designing a marine propeller. Simulations for propeller design might begin with predicting the bare hull resistance and might continue, with increasing complexity, with self-propelled simulations, cavitation simulations and pressure pulse computation. One might end with ship simulations in waves or simulations of manoeuvrability. Each of these applications can be conducted at different levels of computational fidelity and with a variable approximation level; an example of method fidelity for propeller simulations is given in 3.1. Each method embodies different levels of neglected physical effects. The numerical methods applied in this thesis are limited to the highlighted methods (hybrid RANS, lifting surface and lifting line methods). Hybrid RANS simulations are found to be on the edge of being practical in optimisation tasks. In particular, due to the unsteady nature of the rotating propeller, transient simulations are required and simulations might take several weeks, which is too demanding for automated optimisation.

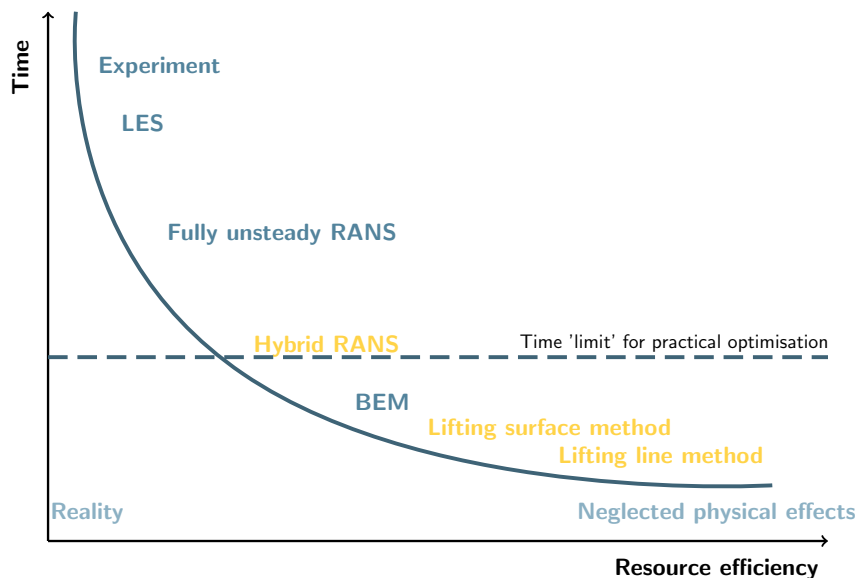


Figure 3.1: Variable fidelity of numerical methods for propeller simulation

3.1 Potential flow propeller analysis model

The prediction of propeller performance using potential methods requires several assumptions, which are applied to simplify the complex flow. The operational domain for a marine propeller is

invariably water, which can be considered incompressible. Consequently, any amount of water that flows into a control volume also flows out at the same time. This can be stated by the continuity equation, which is given in Cartesian coordinates as follows:

$$\frac{\partial u}{\partial x} + \frac{\partial v}{\partial y} + \frac{\partial w}{\partial z} = 0, \quad (3.1)$$

where u, v, w are the velocity components in the x, y, z directions, respectively. Viscous effects are considered to have a marginal impact on the flow because a propeller is operating at a relatively high Reynolds number, which triggers a thin boundary layer (Olsen, 2001). With the additional restriction that the motion of the fluid is irrotational,

$$\nabla \times \mathbf{v} = 0 \quad (3.2)$$

the flow can be described by a scalar velocity potential ϕ . The velocity components are connected through the potential and are derived by

$$\mathbf{v} = \nabla \phi. \quad (3.3)$$

Consequently, the three unknowns (u, v, w) describing the flow are reduced to one (ϕ), which results in a considerable reduction in computational effort. Using equation 3.3 in equation 3.1, the continuity equation simplifies to Laplace's equation

$$\nabla^2 \phi = 0, \quad (3.4)$$

which is solved together with the other boundary conditions for the unknown velocities. Together with Euler's equation of motion, a complete description of the motion of the fluid can be obtained. The Euler equation can be written as

$$\nabla \left(\frac{\partial \phi}{\partial t} + \frac{p}{\rho} - gz + \frac{1}{2} (\nabla \phi)^2 \right) = 0, \quad (3.5)$$

limited to gravity forces and with $\boldsymbol{\omega} = \nabla \times \mathbf{v} = 0$ as a simplification of irrotational flow. By integration, Bernoulli's equation for unsteady potential flow is obtained,

$$\frac{\partial \phi}{\partial t} + \frac{p}{\rho} - gz + \frac{1}{2} (\nabla \phi)^2 = C(t). \quad (3.6)$$

Once Laplace's equation for ϕ is solved, using the boundary conditions, $\mathbf{v} = \nabla \phi$ can be used to calculate the pressure.

The theory established by Rankine (1865) and Froude (1889) and the fundamental works from Kutta (1910), Prandtl (1918), Munk (1919) and Prandtl et al. (1919) show that the flow around a body can be described -with restriction- using only the source, sinks, vortices and dipoles. Generally, due to their circulation properties, vortices are introduced as lift-generating elements, e.g., to model the blade. Sources, on the other hand, can be introduced to represent on-lift-generating bodies, such as sheet cavitation. Lifting line theory is, among the potential methods, the simplest representation of propeller blade geometry. The method originates from the lifting line theory for straight foils by Prandtl, which assumes the wing to be replaced by a single line vortex that creates lift orthogonal to the direction of inflow according to the Kutta-Joukowski theorem $L = \rho \mathbf{v} \times \Gamma$. To satisfy Helmholtz's vortex theorems (mathematically proven by Kelvin's circulation theorems), which states that a vortex element is constant along its length and that it

cannot end in the interior of the fluid, non-lift-generating vortices are introduced at both ends of the wing. They form together with the bound vortex the so-called horseshoe vortex and continue downstream. By introducing several bound vortices that vary in strength from section to section and corresponding free vorticity, the wing representation becomes more realistic. The method is adapted to the marine propeller problem in Lerbs analysis method for a moderately loaded propeller (Lerbs, 1952) and is a vital part of the propeller design procedures to either the optimal circulation distribution or the blade geometry corresponding to a given radial load distribution (Bertram, 2012).

Lifting surface models provide the next most accurate representation of a foil. Throughout this thesis, a numerical method based on the lifting surface theory is applied. The foil is modelled as a continuous distribution of vortices and sources that have to be determined from boundary conditions. First, development for propeller design is presented by Kerwin (1961), where the propeller blade geometry is represented by a lattice of discrete vortices distributed on the mean camber surface. The method is further developed to an analysis method by Cummings (1973) to solve the steady performance of the propeller and by Lee (1979) to predict cavitation and unsteady flow conditions. The vortex segments on the blade (Γ_B) form horseshoe-like vortex loops, whereas the vortices on the shed wake surface (Γ_w) form vortex loops of constant strength. Sources are introduced for a blade thickness distribution (Q_B) and the cavitation (Q_C) (Kerwin et al., 1986). The unknown strengths are determined by applying to the assumptions of potential flow the

- kinetic boundary condition on the foil surface

$$\mathbf{v} \cdot \mathbf{n} = 0, \quad (3.7)$$

which states that the surface is impermeable to the fluid (Lee, 1979). Here, \mathbf{n} is the normal vector to the camber surface, and

- the Kutta condition that prevents infinite velocity at the trailing edge (Lee, 1979), $\nabla\phi < \infty$. From a dynamical perspective, this means that the loading at the trailing edge should vanish, e.g., by applying the Morino-Kutta condition (He, 2010),

$$\Gamma_{w1} = \sum_{L.E.}^{T.E.} \Gamma_B \quad (3.8)$$

Greeley et al. (1982) introduced a vortex wake alignment procedure. The latest versions of the code are named MPUF-3A and include non-linear thickness loading (Kinnas et al., 1993a), hub effects, mid-chord cavitation detection (Kinnas et al., 1989; Griffin, 1998) and non-linear pressure calculation (He, 2010).

Lifting surface methods have a zero thickness blade, which requires a correction at the leading edge for the cavity problem (Kinnas, 1985; Kinnas, 1991) and for the surface friction effects by local section drag coefficients. A more complete representation of the actual blade geometry can be obtained by applying a boundary element method (BEM), e.g., by Fine (1992) and Kinnas et al. (1993b), where the blade is represented through a number of panels whose boundary and control points are located on the blade surface. The boundary conditions are satisfied with a continuous distribution of source sheets and dipoles. In the case of a lift-generating body, a trailing wake with a constant dipole distribution is introduced to satisfy the Kutta condition. This approach provides major advantages regarding the leading edge difficulties and regarding the propeller hub influence. Further BEM provides better possibilities to account for viscosity effects by including integral boundary layer solvers.

3.2 Prediction of propeller cavitation

Turning to the numerical prediction of cavitation, the applied analysis tool MPUF-3A (He et al., 2010, and He et al., 2011) is based on lifting surface theory and in particular on a vortex lattice method, as described above. The cavity determination follows an iterative process, described by Kerwin et al. (1986), and will be outlined in this context briefly.

For the solution of a 2-dimensional cavitating profile section, the cavitation is, similar to the blade thickness, represented by sources. While the thickness is known from the beginning, the cavity source strengths have to be solved for each time step. Their solution requires satisfying the kinematic boundary condition, as described above for a fully wetted propeller blade, as well on the cavity surface. In discretised form, the boundary condition for a cavitating propeller is

$$\sum \Gamma_B \mathbf{v}_\Gamma \cdot \mathbf{n} + \sum Q_B \mathbf{v}_Q \cdot \mathbf{n} + \sum Q_C \mathbf{v}_Q \cdot \mathbf{n} + \sum \Gamma_W \mathbf{v}_\Gamma \cdot \mathbf{n} = \mathbf{v}_{in} \cdot \mathbf{n}, \quad (3.9)$$

where \mathbf{v}_{in} is the inflow velocity vector at the control point, Γ_B and Γ_W are the circulation strengths of the bound and free vortices, and Q_B and Q_C are the magnitudes of the line sources for the cavity and blade thickness (He, 2010). \mathbf{v}_Γ and \mathbf{v}_Q are the velocity vectors induced by each source and vortex loop.

The pressure is, similar to the wetted flow simulation, found by applying Bernoulli's equation, which subsequently determines the occurrence of cavitation when the pressure sags below the prescribed vapour pressure. The resulting dynamic boundary condition forces the pressure on the cavity surface to be equal to the cavity pressure. The final boundary condition on the cavity closure requires that

$$\int_0^l q(x) dx = 0, \quad (3.10)$$

where l denotes the cavity length and $q(x)$ is the cavity source distribution. The cavity thickness h is related to the source strength, such that

$$q(x) = U_\infty \frac{\partial h}{\partial x}; 0 < x < l. \quad (3.11)$$

The three-dimensional solution is found by adjusting the cavity length for all sections at one time step. This is achieved by solving radial stripes of the blade, starting from the hub to the tip and back, until convergence is achieved. One section is thus not a two-dimensional solution, yet it represents a set of stripes in the flow field by combining the undisturbed inflow and the induced flow of the other stripes. The solutions are computed for only one blade (key-blade) to save computational cost. The source and vortex strengths on the other blades are assumed to correspond to those found previously for the key-blade. For each section of a propeller blade, the flow problem in terms of cavity source distribution $q(x)$ and vorticity distribution $\gamma(x)$ can be solved by satisfying the boundary conditions, the Kutta condition and the cavity closure condition. The determination of the cavity source strength follows an unsteady wetted simulation. Cavitation is introduced with a prescribed cavity length $x = l$ and adjusted iteratively until the cavity pressure on the cavity surface agrees with the prescribed value (Kerwin et al., 1986).

Convergence tests of the calculated circulation distribution from MPUF-3A and comparison of first harmonic forces and moments can be found in He et al. (2011) and He (2010). The cavitation prediction is addressed, e.g., in Young et al. (1999) by comparison of cavitation prediction with experimental results and numerical simulations of a panel method. MPUF-3A is developed within

an international consortium on high-speed propulsion (Kinnas, 1996) and constantly validated by the members of the consortium, e.g. Vesting (2010).

3.3 Unsteady propeller forces

The unsteady solution of a cavitating propeller in the wake is obtained subsequent to a start-up procedure. Once steady flow simulations are established, the circumferential variations on the wake are introduced, and the unsteady solution of a fully wetted propeller is found. When a steady state solution in a non-uniform inflow is found, the cavitation is finally introduced until an oscillatory cavitating solution is achieved (Lee, 1979).

The force and moment acting on a physical blade of the propeller can be determined from integrating the pressure jump across the camber surface. For a numerical method, only the pressure distribution on the surface would be required. However, for a lifting surface method, the pressure cannot be integrated properly on the leading edge (Lee, 1979). Thus, an alternative method is to determine the force and moment from the known strengths of singularities. The total force is thus divided into i) force acting on the line source obtained from Lagally's theorem, ii) force acting on the line vortex elements obtained from Kutta-Joukowski's theorem, iii) force following from the change of velocity potential and iv) viscous drag force from a drag coefficient (Lee, 1979). The solution of the strengths of singularities is thus obtained similar to a steady simulation, but for several time steps and with the addition of vortices shed in the wake.

Unsteady propeller forces are caused by circumferential variations in the inflow to the propeller. Unsteady forces are calculated as a combination of steady forces, calculated from circumferential mean inflow and additional fluctuating forces. The three components of the inflow velocity,

$$V_a(x, r, \theta_0) = A_0^a(x, r) + \sum_{n=1}^{\infty} A_n^a(x, r) \cos n, \theta_0 + \sum_{n=1}^{\infty} B_n^a(x, r) \sin n, \theta_0, \quad (3.12a)$$

$$V_r(x, r, \theta_0) = A_0^r(x, r) + \sum_{n=1}^{\infty} A_n^r(x, r) \cos n, \theta_0 + \sum_{n=1}^{\infty} B_n^r(x, r) \sin n, \theta_0, \quad (3.12b)$$

$$V_t(x, r, \theta_0) = A_0^t(x, r) + \sum_{n=1}^{\infty} A_n^t(x, r) \cos n, \theta_0 + \sum_{n=1}^{\infty} B_n^t(x, r) \sin n, \theta_0, \quad (3.12c)$$

are therefore expressed in time and position as the sum of a series of cosine and sine harmonics in a circumferential direction. The steady forces are determined by the zeroth harmonic, whereas the unsteady forces are fluctuating responses to a wake harmonic component with the same frequency and a proportional amplitude but with a phase shift due to the blade geometry (Kerwin et al., 2010).

Each sinusoidal inflow gust induces a sinusoidal force response of the propeller blade. However, the number of blades is crucial for the wake harmonic number and their effect on the total propeller force (Tsakonas et al., 1967). Consequently, the summation of total force only contains those harmonics that are integer multiples of the number of blades (Kerwin et al., 2010), which reads for the axial and tangential blade forces as follows:

$$F_x(\theta_0) = Z [a_0 + a_z \cos Z\theta_0 + a_{2z} \cos 2Z\theta_0 + \dots b_z \sin Z\theta_0 + b_{2z} \sin 2Z\theta_0 + \dots] \quad (3.13a)$$

$$F_z(\theta_0) = \frac{Z}{2} [(a_{z+1} + a_{z-1}) \cos Z\theta_0 + (a_{2z+1} + a_{2z-1}) \cos 2Z\theta_0] \\ + \frac{Z}{2} [(b_{z+1} + b_{z-1}) \cos Z\theta_0 + (b_{2z+1} + b_{2z-1}) \cos 2Z\theta_0]. \quad (3.13b)$$

Typically, the unsteady simulations are conducted with 6-degree increments of shaft rotation when utilising MPUF-3A. The total axial force (T) and the moment (Q) about the x axis, from the tangential blade force, are typically summarised in non-dimensional coefficients

$$K_T = \frac{T}{\rho n^2 D^4} \quad (3.14a)$$

$$K_Q = \frac{Q}{\rho n^2 D^5}, \quad (3.14b)$$

where n is the number of blade revolutions per second. The propeller efficiency behind the hull is related to the propeller forces as

$$\eta_B = \frac{K_T J_S}{K_Q 2\pi}, \quad (3.15)$$

with the advance coefficient

$$J_s = \frac{V_S}{nD}. \quad (3.16)$$

Consequently, the forces have a major impact on the optimisation objective. Particularly, when a required thrust is prescribed, the blade geometry is modified such that the constraints on thrust, cavitation, etc., are fulfilled and the absorbed torque is reduced.

3.4 Propeller-induced pressure pulse

The propeller is the main source of noise and vibration on board ships; the most important source for vibration is thus propeller-induced pressure generated by transient cavitation, which contains multiple blade harmonic components (ISSC, 2006). The consequences of noise and excessive vibration in the ship stern area are damage to sensitive mechanical and electrical equipment, fatigue caused by long-term cycle vibration, and discomfort of crew and passengers (Lee et al., 2006). Additional mass and stiffness in the hull structure is a costly remedy and contradictory to the attempts for lightweight ship structures to control material and operation costs. Consequently, vibration problems need to be addressed by identifying and treating the major sources (Van Wijngaarden, 2011). As one of the main sources, the propeller contributes twofold with forces and moments transmitted through the driving train and pressure fluctuations transmitted to hull surfaces through the surrounding water. The latter is caused by the displacement effect of the propeller blade and its loading and by cavities on the blade, which change rapidly in volume while the blade passes beneath the hull. Both the blade loading and thus the cavitation can be adjusted by modifying the blade geometry, but this typically yields a degradation in propeller efficiency.

The prediction of propeller-induced pressure fluctuations is normally obtained either by empirical formulations, numerical methods or experiments. However, throughout this thesis, a numerical method has been employed to determine the ship-diffracted hull pressure fluctuations (Sun et al., 2007; Kinnas, 1996). The source and the effect of pressure fluctuations are thus modelled separately; no interaction of appendages and propeller is considered. This is advantageous because simplification is admissible for each model. The propeller performance is calculated by the VLM MPUF-3A, as described above, whereas the solution of the ship hull is obtained by a panel method by solving the diffraction potential on the hull. The induced pressure is then calculated from Bernoulli's equation. Hence, the procedure considers one of the prime sources of propeller-induced excitation force: sheet cavitation (Van Wijngaarden, 2011). Potential methods are capable of including sheet cavitation and blade passage for the simulation of the propeller; however, tip vortex cavitation is not considered.

Figure 3.2 (from simulations in paper III) provides an example of the hull model; the method is capable of considering either the exact hull geometry or assuming a hull from given propeller submergence and propeller-hull distance with a flat hull. The panel method for the hull approximated the free surface by a hull image according to Breslin et al. (1982) and applies Green's formula (Kinnas, 1996)

$$2\pi\phi_H + \int G \frac{\partial\phi_H}{\partial\mathbf{n}} - \int \phi_H \frac{\partial G}{\partial\mathbf{n}} = 4\pi\phi_P, \quad (3.17)$$

where:

$G = 1/r$; Green's function,

\mathbf{n} = normal vector to the hull,

ϕ_H = potential on hull,

ϕ_P = potential on hull induced by propeller,

$\frac{\partial\phi_H}{\partial\mathbf{n}} = 0$; kinetic boundary condition.

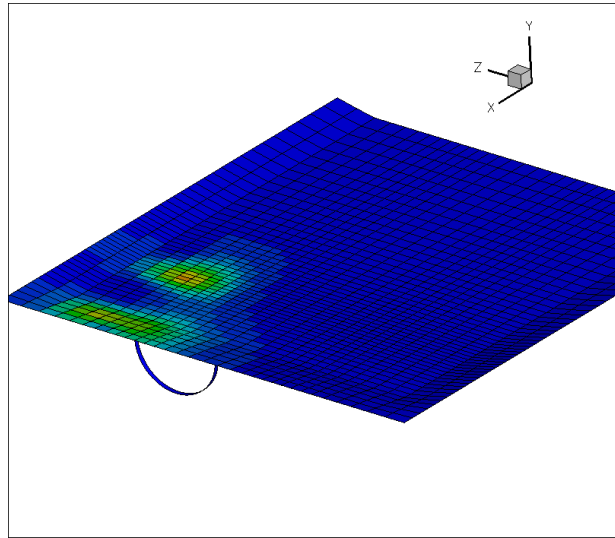


Figure 3.2: Pressure on a dummy hull surface computed from the field point potentials introduced by the propeller

3.5 Hybrid-RANS flow simulation

The flow around the stern of a ship is profoundly affected by the propeller action. The propeller blade geometry therefore has an important influence on its own inflow. This is addressed in paper I, where we investigate the flow, the corresponding forces and propulsion characteristics in a self-propelled propeller optimisation. The approach is a hybrid-RANS flow simulation, where the propeller is simulated by the potential flow code while the entire flow around the stern is solved using the RANS simulation of SHIPFLOW 4.4. This numerical method provides a zonal approach using three types of methods to predict the flow around a body through a division of the domain into three zones according to figure 3.3a: i) a potential-flow solver is applied to solve the inviscid flow around the hull and compute the free-surface in zone 1; ii) a momentum integral method is used to predict the viscous flow in the thin boundary layer on the bow half of the ship in zone 2; and iii) in zone 3, the viscous wake flow is solved using the RANS solver.

In the zonal approach, the inflow conditions to the RANS solver are provided from the boundary layer and potential methods, as described above. The velocity profile of the boundary layer is

introduced to the grid points in the radial direction. Sub grids for a rudder and the propeller are introduced by applying overlapping grids, as shown in figure 3.3b. Because a working propeller will have an asymmetrical effect on the flow, no symmetry plane is considered. The water plane can be treated either as a double model (fsflow) or with a prescribed free surface solution (vfsflow) obtained from the potential flow method. A volume of fluid free surface is not implemented in SHIPFLOW 4.4.

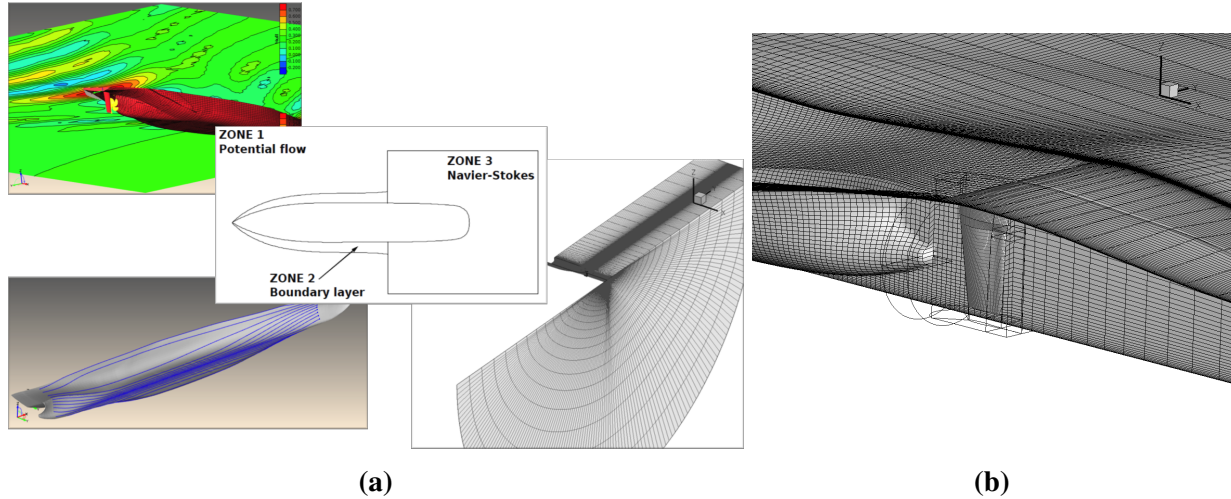


Figure 3.3: Distribution of computational methods within SHIPFLOW's zonal approach (a) and overlapping volume grids at the aft part of the ship with prescribed free surface (b)

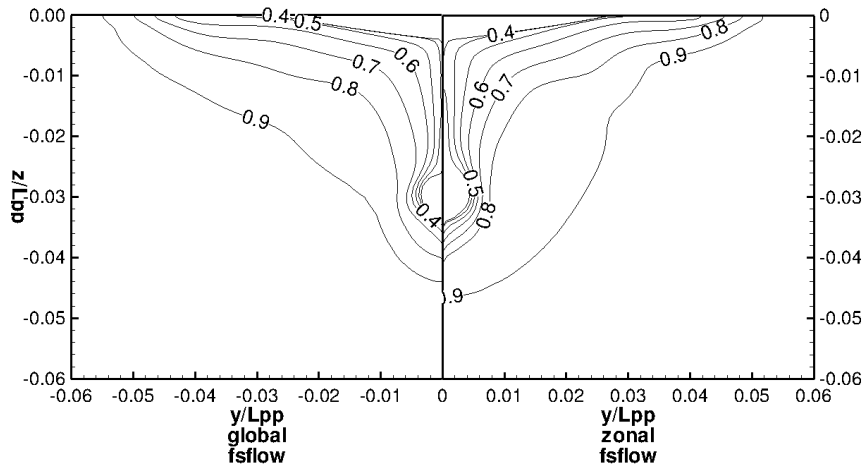
Comparisons of the wake field characteristics between the zonal and the more common global approach, simulating the flow around the entire hull based on a RANS simulation, are investigated for paper I; however, results are omitted in paper I and will be included in this section. The benefit in using the zonal approach is a reduction in computational time because only the stern region of the hull is considered for the computationally expensive RANS simulations, which is beneficial in an optimisation where hundreds of variants will be computed.

The solver for steady incompressible flow is based on a Roe scheme for discretisation of the convective terms, which is an approximate Riemann solver. Because Roe discretisation is only of first-order accuracy, a flux correction is added for defect correction, which is a second-order central differencing scheme. For solving the momentum, pressure and turbulence equations, an alternative direction implicit (ADI) method is utilised to split the finite difference equations and solve them implicitly, whereas the second-order flux corrections are treated explicitly (Regnström, 2007).

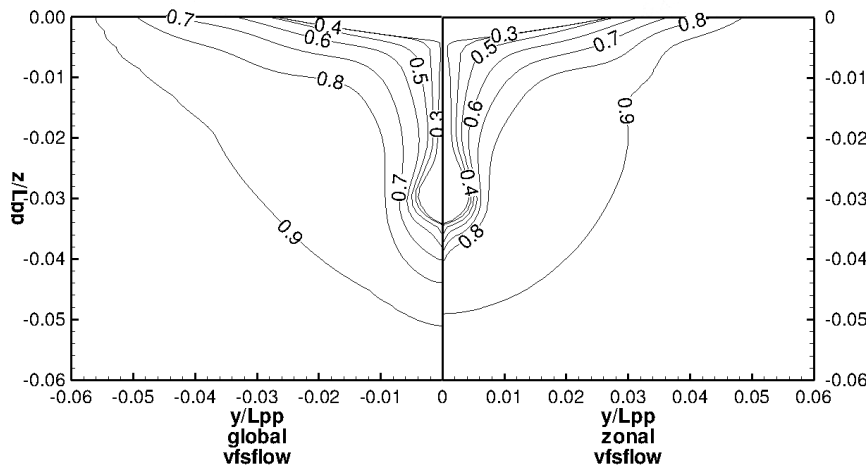
In paper I, all computations are conducted at full scale by applying the explicit algebraic stress model (EASM) for turbulence modelling (Regnström, 2007). The grids are constructed with $y^+ = 0.7$; thus, no wall functions need to be introduced. According to Zou et al. (2010), this turbulence modelling generates the most accurate wake flow.

The domain is a half cylinder with radius $3L_{pp}$ and extends $1.8L_{pp}$ behind the stern and, in the global approach, an inflow is located $0.5L_{pp}$ ahead of the bow. Neumann boundary conditions are used on the outflow of the domain, while on the outer boundary of the cylindrical domain, a zero normal velocity component and zero normal gradient of all other flow quantities are used. On the hull, no-slip conditions are set with zero velocity, k and a pressure gradient. In the global approach, inflow conditions are established with a fixed velocity, k , ω and a zero pressure gradient.

To ascertain that the zonal approach in SHIPFLOW 4.4 yields appropriate results and can be used for propeller-hull interaction studies, simulations of both methods (zonal and global) are compared in a resistance simulation. Moreover, the effect of a double model simulation compared with a prescribed free surface is also tested.



(a)



(b)

Figure 3.4: Axial velocity contour in front of the propeller plane for double model solution (top) and prescribed free surface solution (below)

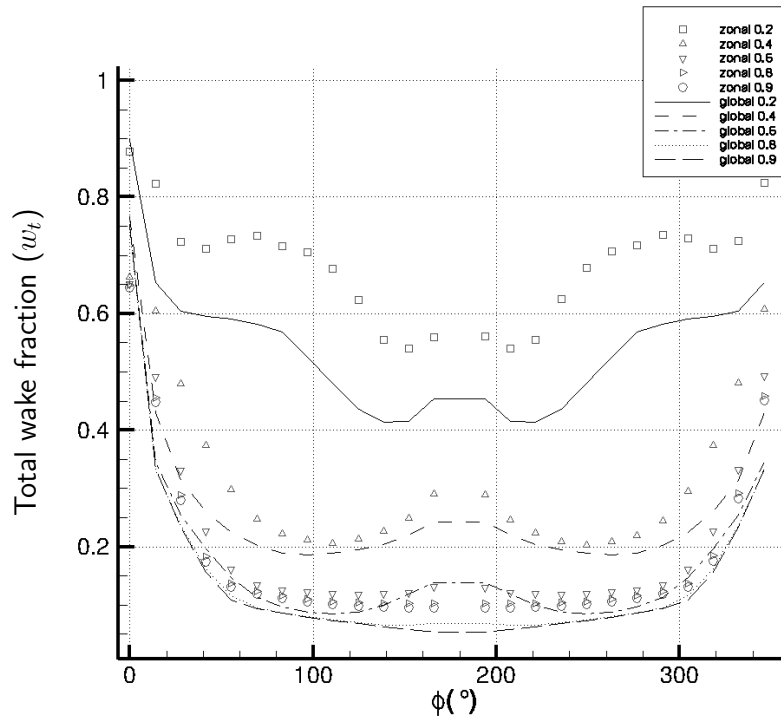
The grid for the global approach contains 6.63 million cells, whereas for the zonal approach, approximately half, 3.42 million cells, are considered sufficient. Figure 3.4 shows the velocity contours in front of the propeller plane. It can be observed that the boundary layer is predicted to be somewhat smaller when using the global approach (left) for all positions and radii when comparing the solutions obtained with the double model simulation (top). This trend is clearest at 180° and can also be observed from figure 3.5, where the circumferential distribution of the total wake fraction is plotted. For the radius $0.2 r/R$, the largest difference can be observed. The differences diminish closer to the 0° position and with larger radii, but even here the wake fraction is still 14% less for the global approach. This observation is in agreement with Zou et al.

(2010), where the global approach tends to underpredict the total wake fraction compared with experimental results.

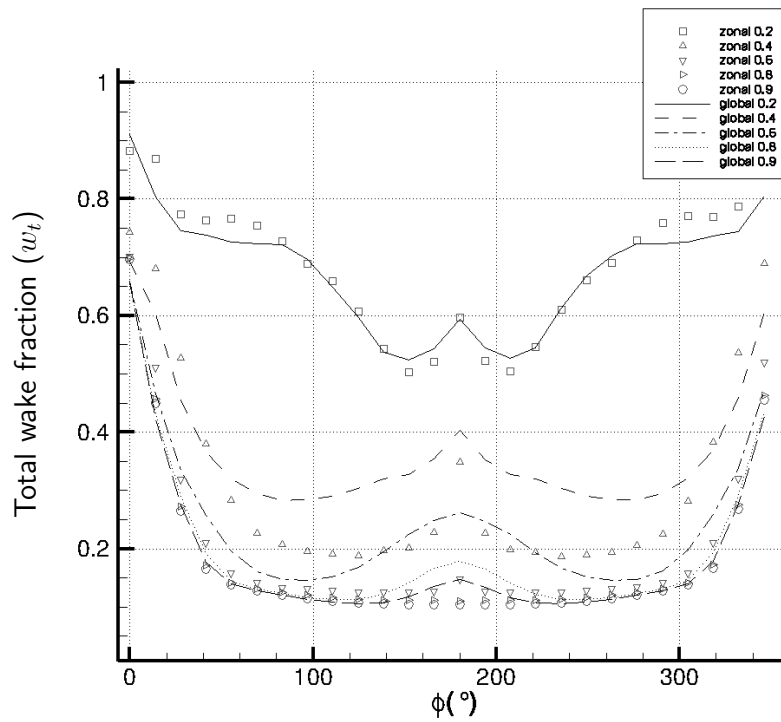
The comparison of the different boundary conditions for the free surface approaches, either prescribed free surface from the potential solution or double model boundary condition, indicates that the prescribed free surface yields smaller differences between the two domain approaches (global or zonal). The maximal difference at the 12 o'clock positions for the outer most radii is approximately 6.5% in the total wake fraction. Both approaches are fairly close in predicting the wake with the free surface boundary condition.

Han (2008) investigated the numerical wake prediction from SHIPFLOW (applying the zonal approach) for the Hamburg test case scenario. The results for four different grid resolutions were compared with experimental data. Han concluded that the general shape and location of the contours of the axial velocity are very similar for the numerical results compared with the experimental measurements. The largest difference is of the same magnitude as the standard deviation of experiments. Thus, Han concluded SHIPFLOW to be sufficiently accurate for capturing most of the flow characteristics with reasonable accuracy.

Visonneau (2010) reviewed local flow analysis for the Gothenburg 2010 workshop and verified SHIPFLOW 4.3 very good agreement with experimental results regarding the axial velocity contours for the KVLCC2 test case. Additionally, the limiting wall streamlines were in good agreement with towing tank results, which confirms the global similarity of the flow.



(a)



(b)

Figure 3.5: Axial velocity contour in front of the propeller plane for double model solution (top) and prescribed free surface solution (below)

4 Optimisation

Optimisation is a concept that applies to numerous situations in everyday life, industrial planning, resource allocation, scheduling, decision making (e.g., robotics) and, of course, in engineering applications. Optimisation is used almost everywhere to either maximise profits or minimise costs. This can be crucial for success or failure in business. The more versatile the concept is, the more diverse are the possible methods for performing optimisation. Optimisation methods can be classified as deterministic- and non-deterministic-based methods, as shown in figure 4.1. However, for both types, the following holds: optimisation is the continuous manipulation of a system to find better solutions with scarce resources. This can be mathematically expressed as the problem of finding a vector $\mathbf{x}^* \in \mathbb{R}$, for which

$$f(\mathbf{x}^*) = \min f(\mathbf{x}) \quad (4.1)$$

subject to

$$g_i(\mathbf{x}^*) \leq 0 \quad i = 1, \dots, I \quad \text{inequality constraints,} \quad (4.2)$$

$$h_j(\mathbf{x}^*) = 0 \quad j = 1, \dots, J \quad \text{equality constraints,} \quad (4.3)$$

$$x_k^l \leq x_k \leq x_k^u \quad k = 1, \dots, K \quad \text{box constraints.} \quad (4.4)$$

This chapter introduces the most common methods of the two classes of optimisation with a particular focus on the selected approaches and provides supplementary information to the description of the methods, as described in the appended papers.

4.1 Deterministic methods

For many applications, the objectives and constraints can be expressed in terms of a mathematical function. If that is the case, deterministic methods are the preferred choice for optimisation. These methods are also referred to as gradient-based or classical optimisation methods and are generally based on the gradient of the objective function. In the case that the objective function cannot be formulated mathematically, as is typically the case in engineering design tasks where the performance evaluation is based on numerical methods, but the use of deterministic methods is still desired, it is common practice to derive a linear approximation with a first-order Taylor series expansion, e.g., Mishima (1996) and Janson et al. (1996). However, such methods require a continuous function to approximate with only minor noise.

1-variable objective functions

The most straightforward conceivable optimisation is a 1-variable optimisation, where only box

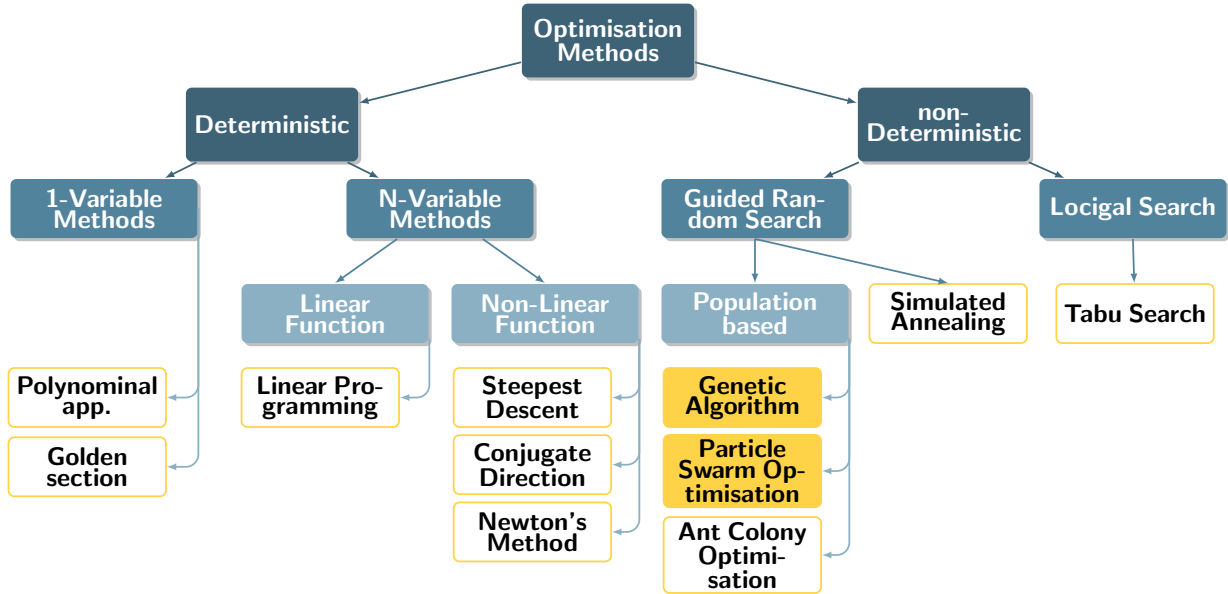


Figure 4.1: Classification of optimisation methods

constraints apply and the objective function depends entirely on a single variable. In this case, the optimum will be found by approximating the objective function with a polynomial through a number of, e.g., calculated objective values. The minimum or maximum is thus determined on the approximation, which requires particular consideration regarding the choice of the polynomial and its coefficients. However, if the objective function is highly non-linear, the approximation will be poor and methods such as the golden section are beneficial; curve fitting is not required, but successive evaluation of the objective function and that $f(x)$ is a unimodal function are required. The technique searches for the extremum, which is known to be in the interval $[x^l, x^u]$ by narrowing the interval. New interior points are found from the formulations of x_1 and x_2 ,

$$x_1 = (1 - \tau)x^l + \tau x^u, \quad (4.5)$$

$$x_2 = \tau x^l + (1 - \tau)x^u, \quad (4.6)$$

with

$$\tau = \frac{3 - \sqrt{5}}{2} = 0.38197. \quad (4.7)$$

The new interval is determined from the evaluation of the objective function at x_1 and x_2 . For the next iteration, the boundaries are redefined and new interior points with the same fraction of τ are introduced.

Optimisation of 1-variable problems is, however, rare in engineering design. For propeller design, a conceivable situation may be the optimisation of the blade pitch for an additional off-design condition in the case of a CPP.

Linear objective functions

Turning to deterministic optimisations with multiple parameters, the methods can generally be categorized as methods for linear and non-linear objective functions. In engineering design, the objective functions are typically non-linear, but it is often possible to linearise the problem by, e.g., Taylor series expansion. The most common approach for solving linear problems is the linear programming method, which considers and requires constraints and takes the matrix form min:

$$F = \mathbf{c}^T \mathbf{x} \quad (4.8)$$

subject to:

$$\mathbf{Ax} = \mathbf{b} \quad (4.9)$$

$$x_i \geq 0 \quad i = 1, \dots, n \quad (4.10)$$

where \mathbf{c} contains the cost coefficients, \mathbf{x} are the decision variables, \mathbf{A} is a matrix for all constraint equation coefficients, and vector \mathbf{b} contains the constraints (Vanderplaats, 2001). There are several algorithms available for solving the linear system of equations, of which the simplex method is the most famous.

Non-linear objective functions

The most common optimisation problems are of the type of non-linear objective functions and can only be solved iteratively from a starting point, with interrogation of the objective function's gradient. The general optimisation strategy is the same for the methods listed in figure 4.1,

$$\mathbf{x}_{i+1} = \mathbf{x}_i + \alpha^* \mathbf{s}_i, \quad (4.11)$$

where \mathbf{x}_i is the current point, the vector \mathbf{s}_i is the search direction to the next location, and α is a scalar for the step size of the movement in the search direction. The gradient $\nabla f(\mathbf{x}_i)$ is calculated to determine the search direction $\mathbf{s}_i = -\nabla f(\mathbf{x}_i)$, which yields the next location \mathbf{x}_{i+1} . The step size α^* represents the optimal step size for the current search direction. The determination is in itself a 1-variable optimisation problem. Equation 4.11 outlines the first-order method *steepest descent*, which only uses the first derivative of f . The *conjugate direction* method is also of the first-order type, but it modifies the search direction based on the concept of conjugate direction, defined as

$$\mathbf{s}_{i+1} = -\nabla f(\mathbf{x}_i) + \beta_i \mathbf{s}_i \quad (4.12)$$

with

$$\beta_i = \frac{\|\nabla f(\mathbf{x}_{i+1})\|^2}{\|\nabla f(\mathbf{x}_i)\|^2}. \quad (4.13)$$

This method dramatically improves the steepest descent in terms of convergence rate and is usually applied following a steepest descent optimisation (Vanderplaats, 2001).

Second-order methods also use the information of the second derivative of the objective function to derive the search direction. The second derivative determines whether a stationary point at \mathbf{x} is a minimum. In the general n -dimensional case, the second derivative is given by the Hessian matrix \mathbf{H} , which is positive definite in the case of a minimum at \mathbf{x} . The search direction derived by Newton's method then reads as

$$\mathbf{s}_i = -\frac{\nabla f(\mathbf{x}_i)}{\nabla^2 f(\mathbf{x}_i)}. \quad (4.14)$$

Algorithms commonly used to solve non-linear optimisation problems are typically based on either one of the listed methods, e.g., the Gauss-Newton algorithm or the Levenberg-Marquardt algorithm. The advantage of these methods is clearly a good convergence; provided that the objective function is quadratic and convex, Newton's methods, for instance, require only one iteration to find the optimum (Vanderplaats, 2001). However, the calculation of the first and second derivatives of the objective function can become very expensive. More problems arise if the objective function is noisy or if constraints are to be applied because the derivative of each constraint function is also required. An alternative deterministic approach utilises sensitivity derivatives of the objective function with respect to the decision variables to determine the direction

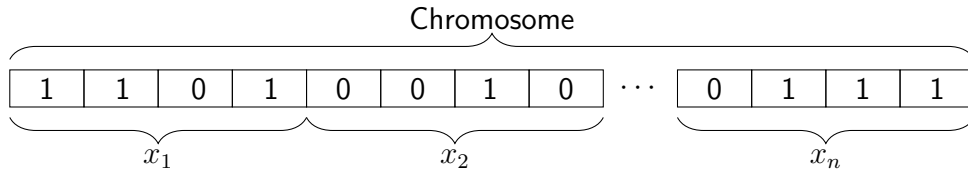


Figure 4.2: Chromosome encoding n variables in a string of four binary digits

of the gradient. The adjoint method combines the residual vector of a flow field solution for a steady flow simulation and the objective function, both differentiated with respect to the decision variables, by an adjoint variable vector. The sensitivity of the objective function with respect to the decision variables is obtained by solving the adjoint variable vector and depends only on the number of decision variables (Sasaki et al., 2001). Thus, only one flow field simulation and the solutions of the adjoint equations yield the required information for the optimiser.

Gradient-based methods can generally obtain optimality with a small number of evaluations. However, the determination of the derivatives may require substantial efforts, and the ability for multi-objective optimisation is generally limited. If the objective function is not convex, these methods are only capable of finding local optima and require several starting points. The adjoint method is very attractive for gradient-based optimisation methods, but it is limited to steady flow simulations and is sensitive to flow instability, such as flow separation.

4.2 Non-deterministic methods

Non-deterministic optimisation methods involve stochastic development during the optimisation. They are typically independent of the gradients and can thus handle noisy or discontinuous objective functions. The development of feasible algorithms is on-going, and new techniques arrive almost daily. These algorithms overcome the shortcomings in classical optimisations, although their origins are not primarily in mathematics. Rather, many of the novel algorithms are inspired by natural phenomena and physics. Simulated annealing, for instance, imitates the process of heating and controlled cooling as in annealing in metallurgy. A slow cooling process is represented in a slow abatement of the probability of accepting a deficient solution in a random search of the design space. Thus, simulated annealing can be categorized as a **guided random search** technique.

Population-based optimisation

Population-based optimisation methods also belong to the guided random search techniques and are typically inspired by nature. The ant colony optimisation (ACO), for instance, copies the behaviour of ants in exploring and exploiting food resources. Similarly, the particle swarm optimisation (PSO) imitates the swarm behaviour related to the motion of, e.g., birds and their ability to search the environment to find food sources and avoid predators by information sharing. In PSO, particles are "flying" through the hyperspace and are controlled by social components for development of the swarm, which contributes to the high search efficiency of the PSO. Both methods have a memory effect from information sharing, which is beneficial in optimisation with constraints.

The most famous population-based optimisation method is the genetic algorithm (GA), which mimics the process during biological evolution to obtain good optimisation solutions. A population is created of variants, where each variant has certain characteristics (phenotype) that are encoded

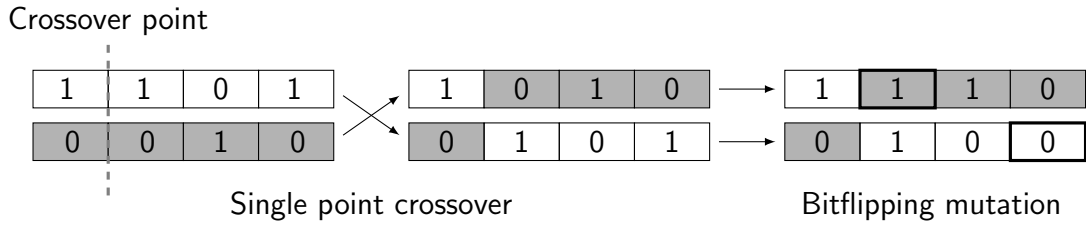


Figure 4.3: Evolving the new child generation for binary encoded variables; crossover of two parent individuals for two child individuals and subsequent mutation

in genes (genotype) of strings of either binary digits (figure 4.2) or floating point numbers. Each of the digits is referred to as a gene, and all genes together form a chromosome, in accordance with the biological terminology. Thus, the characteristics of a variant are obtained by decoding its chromosome. Figure 4.2 depicts an artificial chromosome encoding n variables x_1, x_2, \dots, x_n by binary digits. An objective function for this chromosome could be of type $f(x_1, x_2, \dots, x_n)$. A typical decoding scheme reads

$$x = -d + \frac{2d}{1 - 2^{-k}} \left(2^{-1} g_1 + \dots + 2^{-k} g_k \right) \quad (4.15)$$

for a variable, constrained in the interval $[-d, d]$, with g representing each gene and k being the number of genes decoding one variable.

A GA starts with creating an initial population of N individuals, where each has a chromosome that decodes the individual's phenotype. This is the first generation. After decoding the genes, the actual variables or parameters can be used to evaluate the fitness of each variant. In the next step, the individuals are selected for reproduction. It is essential for the convergence of the algorithm to not always prefer only the fittest individual. In the case of a deterministic selection approach, the currently fittest individual would become dominant and the algorithm converges prematurely to a local optimum. Stagnation can be prevented by applying stochastic selection methods. There are several methods, such as roulette wheel selection (RWS) or tournament selection. In RWS, each individual receives a slot on a roulette wheel proportional to its fitness value; the stopping position of the roulette wheel is then randomly determined. In tournament selection, two individuals are randomly selected from the population, and the individuals with higher fitness are selected with probability p_{tour} , where the tournament selection parameter p_{tour} generally takes a value around 0.7. Hence, the worse individual is selected with a probability of $1 - p_{tour}$.

Once the two individuals are selected by applying one of the selection methods, their genes are combined to create two new individuals. The standard method in GAs is the crossover procedure. Here, a randomly determined crossover point specifies at which gene the chromosomes are separated and reassembled with the counterpart of the reproduction mate. The single point crossover process is shown in figure 4.3 as an example.

Mutation is applied to all newly generated individuals to provide new genetic material. For mutation, some arbitrary genes are selected and mutated with mutation probability p_{mut} . In the case of binary encoding, a mutation means, e.g., bit flipping (figure 4.3) or swapping gene values. When selection, crossover and mutation are completed, there exist two populations, each with N individuals (a new offspring generation and the parent generation). In a basic GA, the new generation replaces the entire parent generation. However, there is always a risk of eliminating the best variants in crossover and mutation processes, which requires elitism as an advanced approach

to maintain already good individuals. In elitism, a few exact copies of the best individuals are selected from the parent generation and placed in the new generation.

Binary encoding of genes features specific characteristics of an implicit probability distribution and characteristics of creating both expanding or contracting crossover (children solutions outside and inside the bounded region by two parents), which is simulated in real value encoding, e.g., by simulated binary crossover (SBX) (Deb et al., 1995). The method presents a spread factor, defined as a non-dimensional ratio of the distance between the two children (c_1, c_2) and two parents (p_1, p_2) in parameter space

$$\beta = \left\| \frac{c_1 - c_2}{p_1 - p_2} \right\|. \quad (4.16)$$

A probability distribution function $\mathcal{P}(\beta)$ is introduced that depends not only on the spread factor but also on a distribution index n

$$\mathcal{P}(\beta) = \begin{cases} 0.5(n+1)\beta^n, & \text{if } \beta \leq 1; \\ 0.5(n+1)\frac{1}{\beta^{n+2}}, & \text{otherwise,} \end{cases} \quad (4.17)$$

which determines where to create the new child solutions due to crossover. Thus, β' is determined from a random number u as the cumulative probability

$$\int_0^{\beta'} \mathcal{P}(\beta) d\beta = u. \quad (4.18)$$

In figure 4.4a, the probability distribution is provided for different distribution indices n and for only one side of the boundary region; a β of 1 corresponds the location of the parent, and accordingly, $\beta \leq 1$ corresponds to a contraction and $\beta > 1$ corresponds to an expansion.

The simulated binary mutation is obtained similarly. The value of one input variable is perturbed by a mutation operator using a polynomial probability distribution (Deb et al., 1996). The mutated value is calculated with the probability distribution

$$\mathcal{P}(\delta) = 0.5(n+1)(1-\delta)^n, \quad (4.19)$$

a random number u and the cumulative probability. Figure 4.4b shows different probability distributions, depending on the distribution index n . The mutated value is finally calculated with the maximum perturbation Δ_{max} as

$$c = p + \delta' \Delta_{max}. \quad (4.20)$$

Thus far, the general genetic algorithm considered only a single objective function for fitness evaluation. However, in some cases, the system must meet more than one objective simultaneously. In such cases, the mathematical description (eqn. 4.1) becomes

$$\min f_l(\mathbf{x}) \quad l = 1, \dots, L \quad (4.21)$$

and a unique solution cannot be identified that simultaneously leads to the optimum in all objectives. A number of methods exist to overcome the problem of possibly conflicting objectives. The classical approach is weighting each objective in a linear combination to become a utility objective

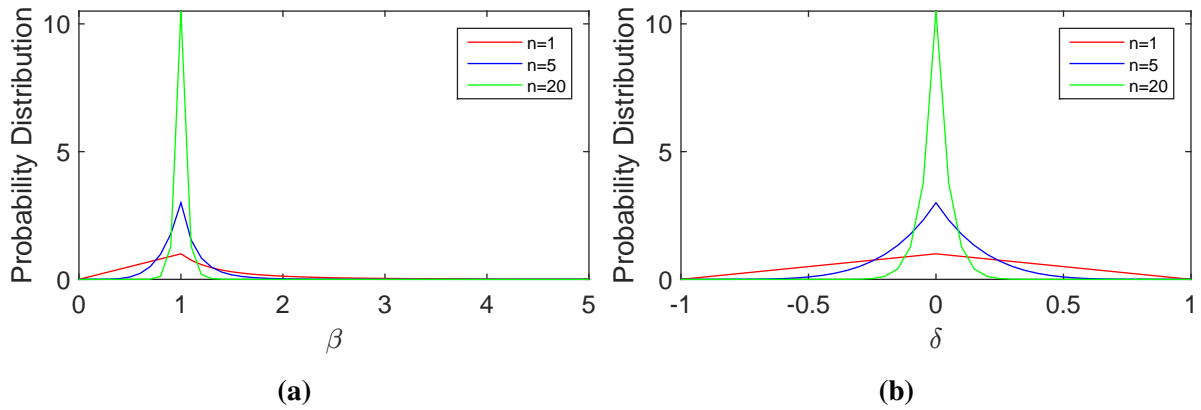


Figure 4.4: Probability distribution in simulated binary genetic algorithm; (a) SBX, (b) polynomial mutation operator

function. However, another approach is to introduce the Pareto dominance concept, where solutions are created and sorted in ascending order according to their level of non-domination. A solution $f_l(\mathbf{x}^*)$ is non-dominated if there does not exist any other solution $f_l(\mathbf{x})$ that is better in at least one of $l = 1, \dots, L$ objectives without a decline in any other objective. Naturally, this leads to a set of solutions along a front identifying the trade-off between the objectives: the Pareto front. Relying on this concept, a ranking-based selection method towards non-dominated methods can be applied.

The genetic algorithm applied throughout this thesis, the non-dominated sorting algorithm II (NSGA-II) (Deb et al., 2002), ranks individuals in the population according to their level of non-domination. Each solution must be assessed to determine its dominated level. The first generation P_0 is typically initiated randomly, but initialization of a deterministic design of experiments is also applied in the attached papers. Prior to creating the first child generation, the solutions are ranked according to their level of domination. In a naive approach, each solution would need to be compared with every other solution to determine whether it is dominated. However, in the NSGA-II, for each solution p , two entities are computed: number of solutions n_p that dominate p and a set of solutions (S_p) that are dominated by p . If there is an individual p for which $n_p = 0$, it is not dominated and will be ranked in the best front, F1. The second front is filled with those solutions, which are in the set S_p (dominated by p) and have a domination count of $n_p = 0$ after it is reduced by one. The third front is determined, again, from solutions that are in the sets S_p of solutions in front F2. This procedure is repeated until all ranks are identified. By classified selection, recombination and mutation, the first child generation C is produced with respect to the rank. Two parents are selected during tournament selection, in which a solution p_1 is selected as a parent before solution p_2 i) if p_1 is feasible and p_2 is not; ii) if both are infeasible but p_1 has a smaller constraint violation; and iii) if p_1 and p_2 are both feasible but p_1 dominates p_2 . In the case that both solutions are feasible and neither dominates the other, the one solution is selected that is located in a less crowded region. Because the individuals in the first rank are now the most efficient solutions, they always receive the most copies (Deb et al., 2002). Offspring and parent generations are combined in a population (R_k) with a population size of $2N$.

All individuals of R_k are sorted according to non-domination rank, as mentioned above. The first rank (F1) now contains the best solutions of the combined population and will be emphasised for the next new population P_k . This new population of size N will be filled with members of F1 and, if $F1 < N$, successively with the best solutions of the sets F2 and F3 until no more individuals can be accommodated. The individuals of the last non-dominated front, which do not entirely fit in

P_k , are sorted using the crowded distance operator. The crowded operator introduced by Deb et al. (2002) is based on a density of solution estimations by calculating the average distance between the solutions in each direction of the objectives. Solutions located in a less crowded region are considered preferable. This enhances the search and avoids premature convergence.

GAs are found to be quite robust in various applications. This arises from different starting points distributed in the design space and random variation through mutation operations. Premature convergence can further be improved through varying mutations depending on the diversity of the population, mating restrictions to avoid incest or island models with sub-populations.

The favoured optimisation methods used in this thesis are the population-based methods. They are readily applicable and flexible for propeller optimisation with changing constraints and are capable of multi-objective optimisation without prescribed objective relations. The consideration of constraints can be controlled in these methods, for instance, to allow for infeasibility, as described in paper V. A further advantage of population-based optimisation algorithms is the population-wise evaluation of design alternatives, which enables parallel computation of variants within one population before the algorithm assesses them.

4.3 Meta-models

Meta-models are aiming to replace computationally expensive methods or even experiments with interpolation or approximation approaches by creating a function which can approximate the response to an unknown input rapidly. A set of known solutions is, however, required to fit the multi-dimensional surface to the system behaviour. Typically, these samples are created in a design of experiment (DOE) sampling and require a sufficient representation of the design space. A wide range of response methods exist, such as parametric functions (linear, polynomial or exponential), interpolation on known samples, and neural networks. The most prominent models are probably least squares fitting of a first-order polynomial and second-order polynomial by Box et al. (1951)

$$f(x) = \beta_0 + \sum_{i=1}^k \beta_i x_i \quad (4.22)$$

and

$$f(x) = \beta_0 + \sum_{i=1}^k \beta_i x_i + \sum_{i=1}^k \beta_{ii} x_i^2 + \sum_{i=1, i < j}^k \sum_{j=1}^k \beta_{ij} x_i x_j. \quad (4.23)$$

In this manner, the actual response $y(x) = f(x) + \varepsilon$ is found with an estimation error ε , which is assumed to be normally distributed with mean zero. Polynomials are flexible and can be applied to a wide range of curvatures. However, the selection of the polynomial degree is crucial for the shape of the response surface, and known points are not necessarily approximated exactly.

The methods for meta-models considered in this thesis are Kriging interpolation and neural network methodologies. The methods and results are discussed in paper II; in particular, with regard to the objectives performed, the Kriging approach is superior. There are certainly more methods available, e.g., the radial basis function (RBF) and the RBF neural network are frequently used meta-models (e.g., Ellbrant (2014)). Costa et al. (1999) compared the performance of Kriging and RBF networks with Gaussian kernels and concluded that the performance differs significantly; although both of the predictors share the same structure, higher accuracy of the estimations is obtained from Kriging. Backlund et al. (2010) investigated Kriging, BRF and support vector regression as meta-models for an engineering design problem, with a particular focus on the model

construction and prediction time; it was concluded that the Kriging performs better in terms of construction time and that the RBF is faster in predicting new data points. Chandrashekarappa et al. (2007) compared RBF and Kriging for aerodynamic optimisation tasks; on a 1-dimensional test function, the RBF is more accurate, whereas the Kriging performs better on a 2-dimensional test function, particularly towards the domain boundaries. In the case of an 8-dimensional aerodynamics problem, both prediction methods perform similarly (Chandrashekarappa et al., 2007).

Regardless of which meta-model or response surface is used, all approaches use statistical methods and approximate an unknown relation given by a discrete set of samples. Thus, an optimum solution found by any meta-model is always subject to uncertainty on top of the uncertainty in the method applied to predict the samples (e.g., experimental uncertainty or uncertainty of numerical methods). The accuracy also depends on the density and distribution of sample variants in the design space. This is a crucial factor in the approach of applying meta-models. If the number of samples is coarsely distributed, the optimisation algorithm will be unable to find an optimal solution based on the meta-model. Otherwise, if many samples are needed, the overall time advantage is lost. Thus, either a sophisticated method needs to be applied that provide guidelines to divide the design space to minimise the required inputs, e.g., orthogonal arrays as suggested by Peri (2009), or meta-models need to be assisted by continuously improving them with new computed variants during the optimisation.

The general conclusion of paper II is that optimisation based entirely on meta-models is insufficient but that meta-models are capable of capturing the correct trends. This conclusion motivates the application and development of optimisation algorithms that are assisted by meta-model estimations to reduce the overall optimisation lead time. In figure 4.5, a general approach for such assisted optimisation in propeller design is outlined in a macroscopic scale without details on the optimisation algorithm itself. However, it is assumed that the meta-model only surrogates the analysis tools of the propeller. The process begins with an initial design (see chapter 2.2), e.g., from the designer's database, and enters a geometry modification module. The application of potential propeller analysis tools is efficiently accomplished by modification of geometry distribution curves. Once the new geometry is created, an algorithm decides to use either the meta-models or simulation by the analysis module. The decision can be related to the training status of the meta-model or prescribed. The analysis module is used to provide training data for the meta-model, which are stored in a separate archive. In the case where the propeller variant is to be evaluated by the meta-model, the meta-model needs to be built or rebuilt with the latest archive. It is suggested to apply either a meta-model that assesses the n-dimensional parameter neighbourhood of a variant to find a possibly better solution and then evaluate that with calculations or to evaluate the design exclusively with the meta-model. In the optimisations conducted in this thesis, the decision is always prescribed. However, the algorithm may also base this on, e.g., the training status of the meta-model or the progress of the optimisation. Once the hydrodynamic evaluation of the propeller variant is completed, the optimisation proceeds with the evaluation of, e.g., blade strength and other limitations or objectives. In paper V, we describe how this procedure, as outlined in figure 4.5, is implemented together with the NSGA-II, which is rewritten into two meta-model-assisted algorithms (AS NSGA-II and SANA NSGA-II).

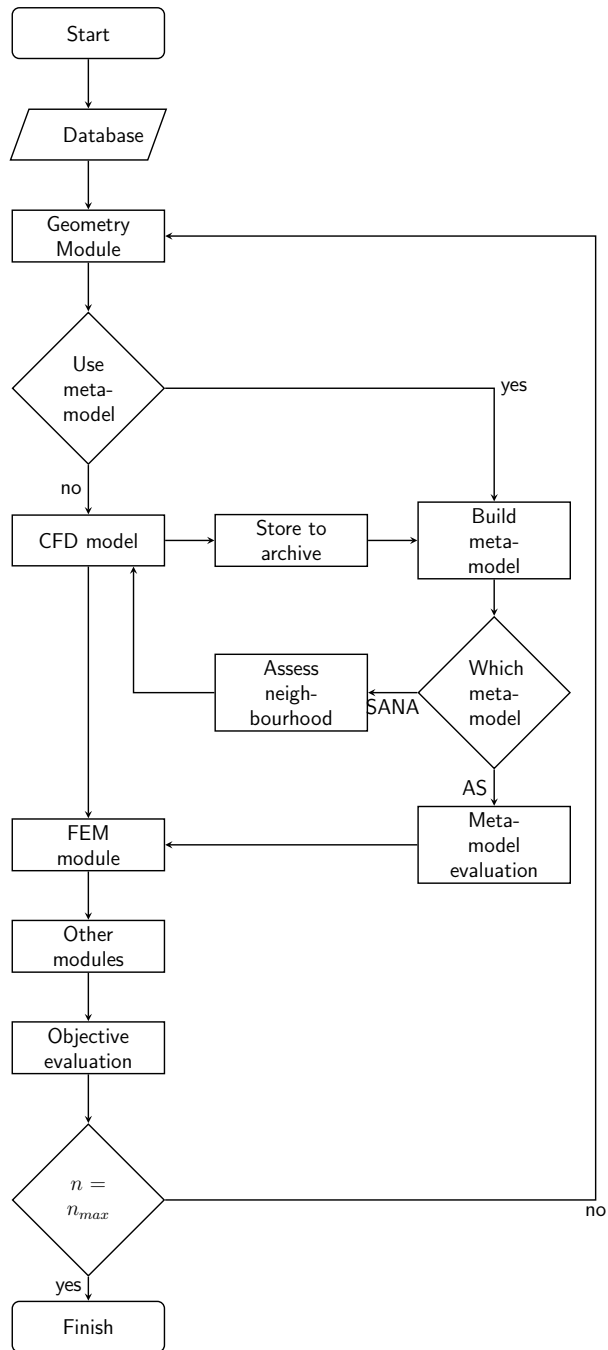


Figure 4.5: Macroscopic propeller optimisation process involving meta-model evaluation

5 Summary of the work in the appended papers

5.1 Paper I

Paper I presents the optimisation of propeller blade geometry in interaction with the ship and consideration of sheet cavitation prediction. In behind conditions, the effect of the propeller on the flow field around the stern of the ship is taken into account, and the effect of design variations of the propeller blade on the flow is studied. In this paper, we initiate the discussion on cavity shape constraints, motivated by the concept of large-scale cavities that develop into focusing cavities and result in a higher risk for erosion (Bark et al., 2004) and (Foeth, 2008).

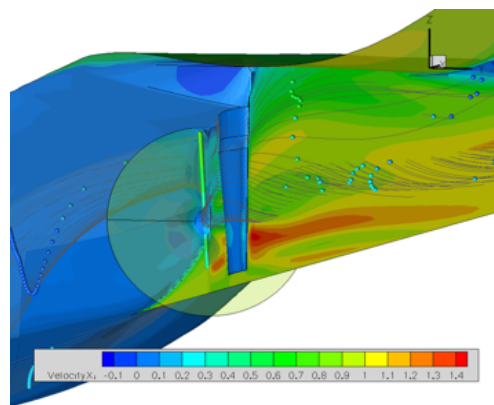
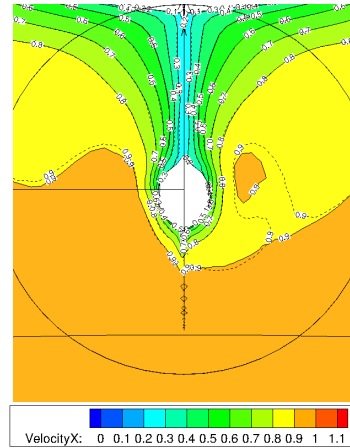
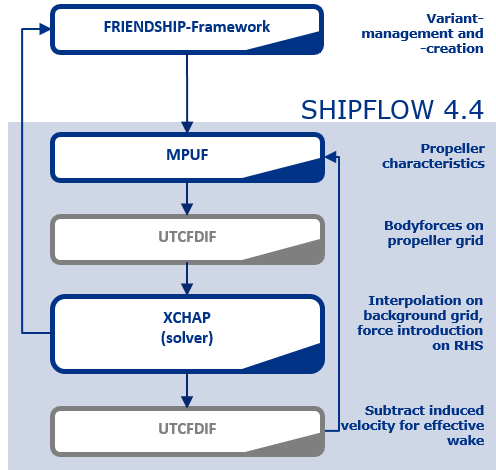


Figure 5.1: *Hybrid RANS propeller simulation, where the propeller forces are embedded to the flow around the aft ship*

The propeller performance itself is calculated by the potential flow method, whereas the flow around the hull, including the rudder, is simulated by RANS flow simulations. In an iterative update procedure (figure 5.2a), the inflow to the propeller is taken from the flow field, reduced by the induced propeller velocities and used as an input for the propeller simulation. Subsequently, the propeller forces are interpolated on an embedded cylindrical propeller grid, which are then added as volume forces to the right-hand side of the RANSE solver. The ship is thus simulated in a self-propelled manner with an equality restriction on the ship's speed. The equilibrium is enhanced by adjusting the rotational speed of the propeller.

For the multi-objective optimisation, a genetic optimisation algorithm is used to maximise the propeller efficiency while minimising the propeller-induced pressure pulses. The objective on the

pressure pulses is considered to be a minimisation of the root-mean-squared amplitude of the first three blade harmonic frequency components, which are computed by field point potentials on a set of points above the propeller shaft. Geometry variations are conducted by applying modifications to the initial design in terms of changing the chord, camber, skew and pitch parameter distribution curves.



(a) Iterative update procedure to determine the effective wake (b) Axial velocity distribution of two blade alternatives with contradictory performance in p

Figure 5.2

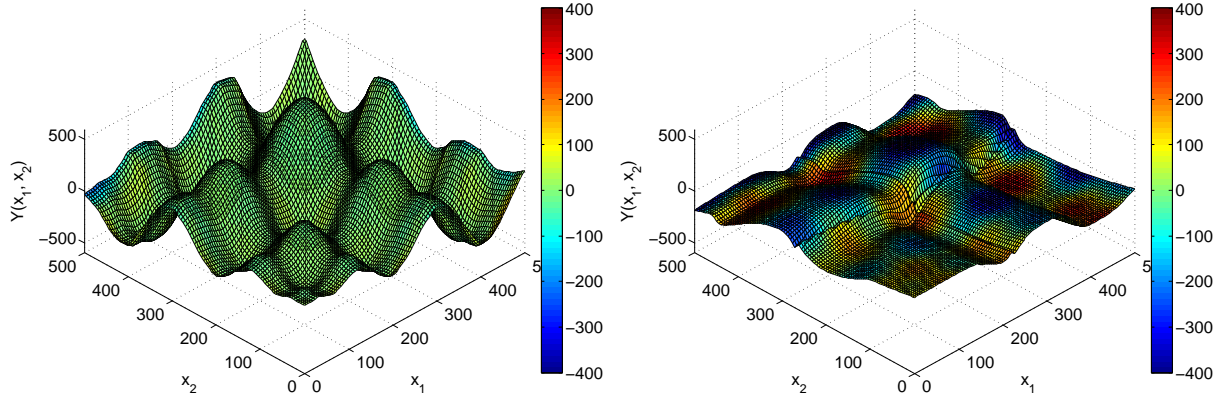
This paper reveals a considerable difference in the axial flow velocity between the blade variants of the optimisation. In figure 5.2b, the inflow in front of the propeller plane is given for the best performing variant in comparison to a variant with similar performance in η but opposite performance in p and cavitation volume (dashed lines in figure 5.2b).

Even if a strict convergence of the optimisation is not obtained, the variants with the best performance share similar geometries, with higher loads at the mid-span region due to an increase in pitch and camber. Although the hull and propeller geometries are different, the development agrees well with the earlier results reported by Han et al. (2006). Paper I concludes that the pressure pulse objective depends strongly on the cavity shape and that the constraints on cavity shape need refinement.

5.2 Paper II

Paper II discusses meta-models for propeller optimisation problems. Three different approaches are explored, namely, Kriging, feed forward neural network and cascade correlation neural network, to replace computationally expensive methods by approximation or interpolation methods. All methods promise feasible accuracy and capability to predict non-linear relations, and each of them has already been applied in marine applications. However, the aim is to apply these methods to predict detailed information regarding the propeller performance, including cavitation. This has not been addressed before in previous studies.

Initially, three approaches are tested to estimate the Schwefel test function. Only the Kriging (figure 5.3a) and feed forward neural networks (FFNN) perform satisfactorily. While the FFNN provides a minor deviation from the original function at the boundaries, the cascade correlation neural network (CCNN) fails to estimate the surface. Further investigations in paper II on a



(a) Application of Kriging meta-model to estimate the Schwefel test function (b) Application of cascade correlation neural network meta-model to estimate the Schwefel test function

Figure 5.3: Meta-model performance in estimation of the test function; surfaces are coloured according to the error on the analytical surface

propeller test case are therefore restricted to the Kriging approach and two versions of FFNN.

The meta-models are applied to estimate the performance of a test propeller and are used to optimise the propeller with respect to maximising the propeller efficiency while minimising the propeller-induced pressure pulses and considering constraints on cavitation. Unlike in paper I, the simulations are conducted exclusively with a fixed effective wake and no interaction effects. The cavity shape constraints are refined in paper II, as a consequence of the findings in paper I, to locally monitor and restrain cavities. In particular, we introduce cavity thickness constraints at the blade tip and calculate and constrain the maximum cavity centroid in the chord-wise direction, as well as the maximal change in cavitation volume between two consecutive time steps.

Paper II reveals, from a comparison of the meta-model estimates on the performance of a propeller, that each model has its weaknesses, but the FFNNs perform predominantly insufficiently except for the prediction of the cavity centroid constraint. The Kriging, on the other hand, fails in predicting the cavity centroid. Consequently, a combined meta-model approach, which selects the best model for each quantity, is introduced to estimate the propeller performance. Additionally, two optimisation strategies are tested: i) optimisation entirely with the estimated results and ii) optimisation with the estimated results to find the global optimum and subsequently start from the found location with a local search method associated with the calculated results.

In figure 5.4a, the correlation between the estimated and calculated results of the best variants obtained from the optimisation reveals a good agreement for the efficiency estimation. The pressure pulse estimations, however, deviate from the computed results, and in the case of the cavitation constraints, only correct trends could be captured from the meta-models. The optimised solutions are still considerably better than the input samples and provide a significant improvement regarding the cavity shape, which is transformed from a mid-chord cavitation towards attached sheet cavitation (figures 5.4b and 5.4c).

The second paper concludes that the meta-models are beneficial in lead time and are able to provide the correct trends for geometrical modifications in an optimisation. However, an optimisation based entirely on the meta-model estimations is too sensitive for the samples used to create

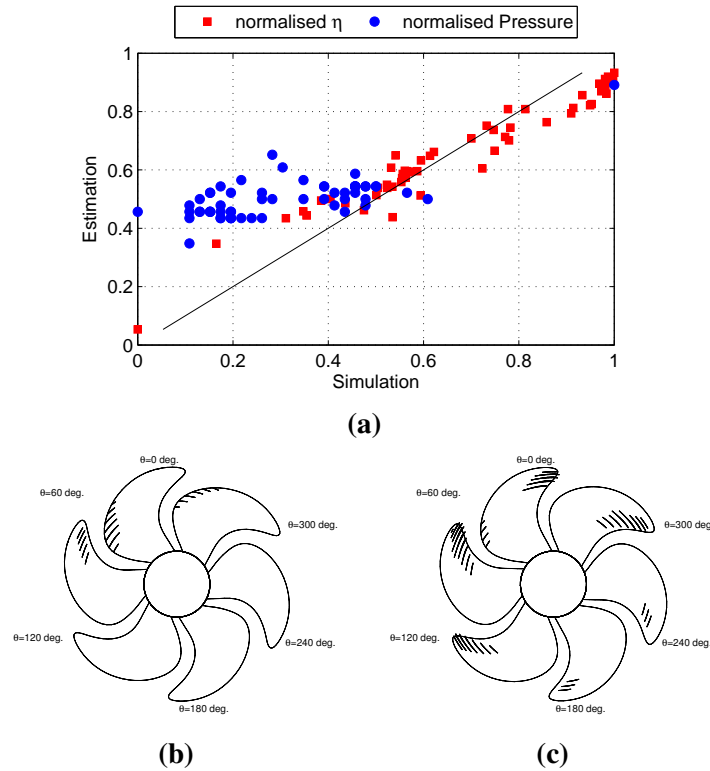


Figure 5.4: (a) Correlation between meta-model estimates and calculated results, (b) cavitation predicted best design based on meta-model optimisation, (c) cavitation predicted baseline design

the meta-model. Hence, an optimisation based solely on a meta-model is not recommended; rather, a hybrid approach in which the meta-model is adjusted during the optimisation is recommended.

5.3 Paper III

The parameter influence for a propeller that is evaluated for multiple operating condition is studied in paper III. The propeller's efficiency is maximised for the propeller operating in open water conditions, while the same propeller is optimised for minimum pressure pulses and subject to sheet cavitation operating in a fixed effective wake. Additionally, regarding the cavity shape constraints, classification rules for 'Calculation of Marine Propellers' according to Det Norske Veritas (DNV, 2012) have to be fulfilled.

In total, two optimisations are conducted. The first optimisation (optimisation 1) uses all 11 input parameters, while the second optimisation uses a reduced set of input parameters according to the results of a sensitivity analysis. The extended FAST (Fourier amplitude sensitivity test) is employed to calculate the sensitivity indices for each parameter and considers the interaction effects between parameters. Parameters with high impact on the objectives are accordingly the applied camber and skew modifications. The camber influences the cavitation volume and the major parameter. The cavitation on the blade tip is, according to the sensitivity analysis, controlled by the pitch and the blade thickness at the tip. The influence of chord, however, is not entirely resolved by the sensitivity analysis.

The optimisations reveal that similar improvements are possible through the applied geometry variations with and without reduced input parameters. However, the convergence is improved with

less input parameters, which require fewer evaluations and therefore reduces the optimisation lead time. The geometries of the best performing solutions from optimisation 1 and the converged solutions of optimisation 2 follow the same trend, but only the chord parameters are excluded in optimisation 2. All the designs incorporate a reduction of the maximal cavity volume. However, for most of the variants with improved efficiency, there is a shift in cavitation volume evident rather than an overall reduction, as shown in figure 5.5. The volume is reduced at the blade position with maximal volume but increased at later blade positions.

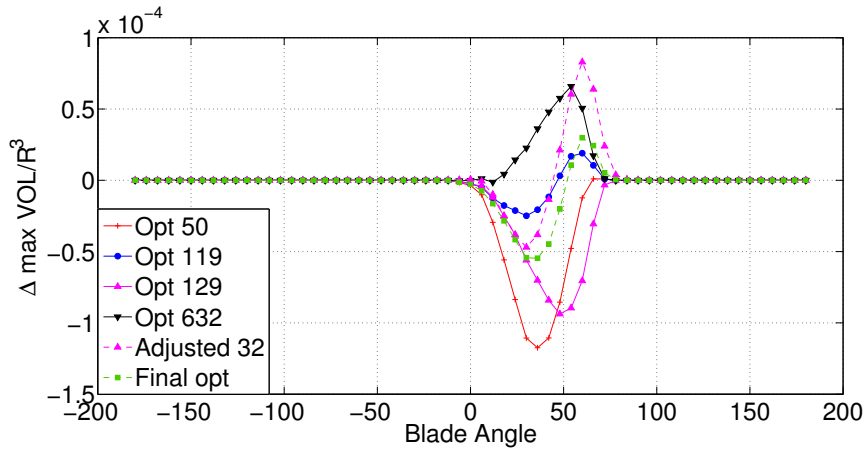


Figure 5.5: Cavity volume at each blade position referenced to the cavity volume of the baseline design. Blade position with the maximal volume: 48

5.4 Paper IV

This paper addresses improving and evaluating the performance of two population-based algorithm approaches for automated engineering design optimisation. In paper IV, the particle swarm algorithm (PSO) is adapted towards multi-objective optimisation and constraint handling for use in propeller design. Three different approaches for the multi-objective handling are investigated, and the results are compared with the well-established NSGA-II genetic algorithm as a benchmark. Test optimisations are conducted on four commercial propeller designs for different ship types. Special consideration is given to a classified assessment of the optimisation outcome in terms of performance, convergence and geometry by interrogating the median values of parameter, objective and decision variables.

The three versions of the multi-objective PSO algorithm differ in the use of disturbance (either mutation on particle velocity or particle position) and nomination routine of the best solutions. Two of the proposed PSO algorithms utilise either a pure single objective or an aggregate objective function. The corresponding results show partly premature convergence and convergence towards an improvement of only one of the objectives. Therefore, tournament selection based on the non-dominated rank and crowded distance is introduced to the algorithm (PSOt) to maintain a selection pressure towards non-dominated solutions as the nominated best solutions for the PSOs cognitive and social contributions. With the PSOt algorithm, a separate archive of personal best solutions is introduced, which are continuously updated regarding their non-dominated ranks and crowded distances with respect to setting the bests in relation with the latest swarm time step.

Particular cavity shape constraints, despite cavitation volume and cavitation length, are not applied in paper IV. However, special consideration is given to the handling of constraints. Because a designer is possibly interested in designs that perform excellent although they might

be marginally infeasible, such a design outlines the next design step. A design that performs insufficiently regarding a single constraint is possibly good regarding other constraints or the objectives and should not necessarily be removed from the population. Thus, in paper IV, each result of a constraint function $g_i(x)$ is assigned with a constraint violation, which is relative to the maximum or minimum values of $g_i(x)$ in the current population. Using the aggregated constraint violation measure (CVM) enables a solution to balance a violation in one constraint by one or more positive (feasible) constraint violations. Accordingly, a CVM becomes negative in the case of a violation of the constraint, zero if the constraint value matches the constraint limit, and positive if the constraint value exceeds the limit. In this way, it is possible to consider solutions that are infeasible in one or more constraints but still feasible in other constraints.

The evaluation of the optimisation results focuses on the median results per generation and the development of the Pareto front, which describes the main development of the objectives or parameters clearly. The proposed multi-objective PSO algorithms are generally lagging behind the NSGA-II results in terms of finding the best trade-off quality. However, the proposed PSOt yields comparable results, converges earlier and enhances the solution in terms of constraint violations. In two of the propeller test cases, the PSOt outperforms the benchmark algorithm (NSGA-II) based on the Pareto solutions. It also creates comparable feasible sets of solutions and additionally manages to make violations of an active constraint preferable. Thus, PSOt is highly suitable in constrained propeller optimisation, particularly in an early design phase.

5.5 Paper V

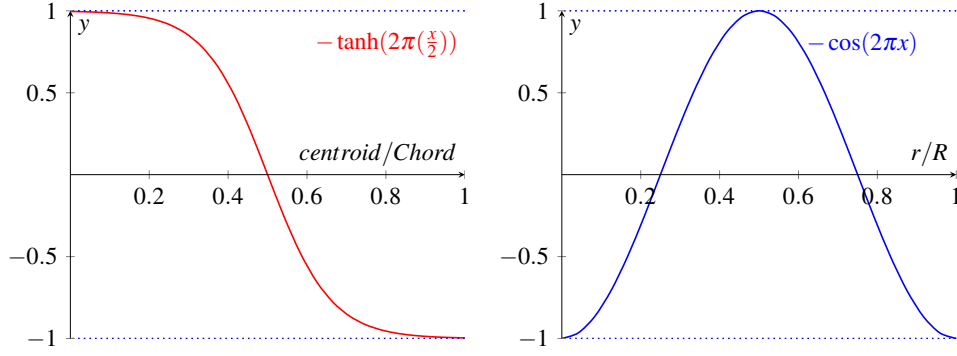
The purpose of paper V is to improve the commonly used population-based algorithms (NSGA-II and PSO) towards the application of marine propeller design. The extensions to three algorithms are outlined utilising other meta-models, adapted constraints and modified constraints handling. On one test propeller, 13 optimisation strategies, as combinations of algorithms, geometry modifications, and constraint and objective selections, are tested. New cavitation constraints based on potential flow prediction are proposed for the cavitation centroid and the cavity closure line.

Based on the NSGA-II, two algorithms are extended to utilise the Kriging meta-model approach to predict objective and constraint values, to improve the algorithm by either enhancing the convergence or reducing the optimisation lead time. To reduce the lead time, we propose the adaptive surrogate NSGA-II (AS NSGA-II), which evaluates the variants on the surrogate method and updates the meta-model frequently while the optimisation proceeds. The second algorithm is the surrogate-assisted neighbourhood assessment NSGA-II (SANA NSGA-II), which assesses the neighbourhood of each solution candidate. For each solution candidate, several solutions in the neighbourhood are evaluated utilising the meta-model, and the best is returned to relieve the candidate, which is finally evaluated using the calculated results.

The cavity shape constraints are finalised in paper V by introducing harm-factors on the cavity closure line and the cavity centroid constraints. The closure line is measured at each blade position and compared with a normalised convex benchmark closure line curve. The difference between the given curve and the section-wise cavity length is compared as the root-mean-square (RMS) error. This is performed for each blade position, and eventually, the blade with the smallest RMS error is selected and returned because it provides the highest similarity with the convex shape.

The cavity centroid harm-factor is designed to rate the position of the maximum chord-wise centroid of a cavity section on the blade. Therefore, the blade is divided into harmless and harmful

sectors. If the maximum cavity centroid is at a downstream location, at the blade tip or at the blade root, it is associated with a negative value, a penalty. Conversely, if the centroid is located at a small portion of the chord length or at the span-wise centre of the blade, it will be associated with a positive value, a benefit. Figure 5.6 shows the assignment of the harm-factor according to a hyperbolic tangent function for the centroid location in the chord-wise direction and a cosine function in the radial direction. Thus, the centroid harm-factor comprises the general location of cavity shape in the vicinity of the key-blade.



(a) Harm-factor for chord-wise location (b) Harm-factor for span-wise location

Figure 5.6: Calculation of the harm-factor follows a tanh distribution in chord-wise direction and a cos distribution in radial direction

To modify the blade geometry locally, an iterative routine to indirectly shift the B-spline parameter distribution curves is introduced. An offset to the B-spline curve control points is initialised by modifying two 4th-order Bézier curves. The desired parameter value is iteratively achieved and stops the modification of the Bézier curves when the parameter curve passes the desired point. In the process, a width factor determines the span-wise perturbation of the parameter curve and applies smooth modifications to the original curve.

The assessment is classified into three categories: *performance*, *convergence* and *constraints*. This classification facilitates the rating of the optimisation among each other and provides a measure for the overall optimisation achievement. Two algorithms of the proposed modifications (PSO and SANA NSGA-II) perform exceptionally and improve the performance significantly. They converge strictly towards the Pareto front and provide, rapidly after only 10 generations, a positive CVM median with the smallest deviation of the thrust coefficient. The cavity shape constraints yield more solutions with higher pressure pulse improvements and control the cavity shape and thus the objectives and geometry development. Local curve modification achieves the intended cavitation modification. The three algorithms (NSGA-II, AS NSGA-II and SANA NSGA-II) converge to the same geometries and indicate an advantage of the AS NSGA-II, which reduces the lead time by a factor of five.

Two of the proposed algorithms (PSO and SANA NSGA-II) perform well compared to the NSGA-II, particularly with regard to constraint compliance, when applied in connection with standard parameters for the geometry distribution curves. They are advantageous in an early design phase. In an optimisation with local blade modifications, the AS NSGA-II yields comparable optimisation results and is hence advantageous due to the short lead time. The cavity shape constraints evidently improved the cavitation and thereby enhanced the pressure pulse objective. Paper V concludes that the applied modifications to the algorithms are beneficial in marine

propeller design but that propeller design is seldom possible in a single-step approach. The outlined strategies need to be used in a systematic optimisation series with an intermediate assessment by an expert.

5.6 Paper VI

The purpose of paper VI is to test the proposed optimisation strategies and algorithms on a broader range of propellers for different applications and with different cavitation patterns. A two-stage optimisation procedure is outlined for marine propellers (figure 5.7), where the geometry is first modified by parameterised geometry distribution curves to gather knowledge of the test case. The first optimisation set-up depends on the case in terms of constraints, objectives, and parameter and algorithm selection. In paper VI, several strategies and algorithms for the primary optimisation are assessed, and their influence on the optimisation performance is evaluated. A supporting optimisation aims to improve the design by locally changing the geometry based on the results of the first optimisation.

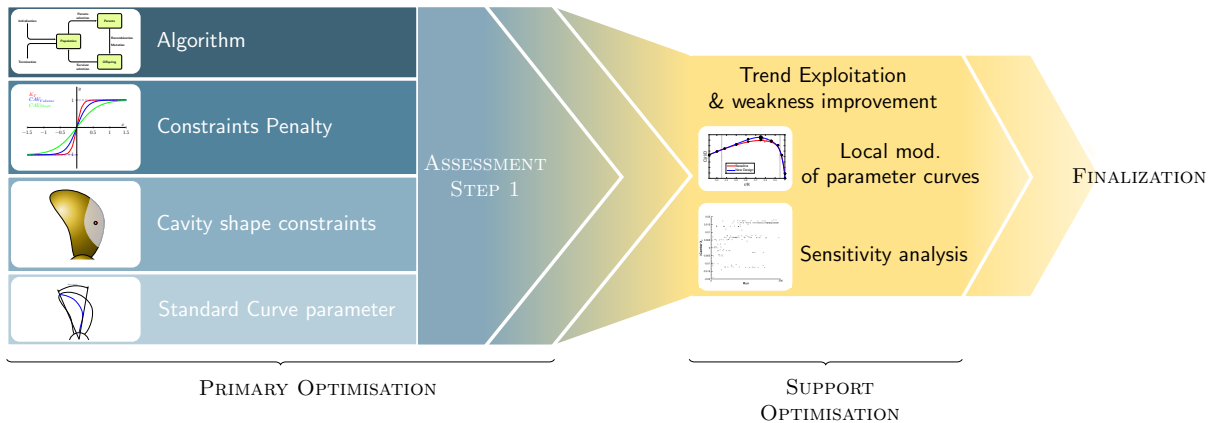


Figure 5.7: Two-stage optimisation procedure for multi-disciplinary marine propeller blade optimisation

Frequently, the NSGA-II provides the best compromise between two objectives and converges in both towards an approximation with the fewest variations. However, compliance with the constraints is frequently insufficient. The proposed PSO and SANA NSGA-II algorithms both perform particularly well in terms of adherence to constraints. The PSO is characterised, beyond the constraints compliance, by a rapid convergence. The cavity shape constraint on the cavity centroid harm-factor and the sheet thickness constraints perform well and manage to control the optimisation in the expected manner. In particular, during the support optimisation, designs could be improved regarding cavitation utilising the shape constraints.

The different approaches are evaluated, and the final results of the automated optimisation toolbox are compared with the designs generated in a manual design process. The automated optimisation provides, in comparison with the manually designed propellers (according to the established design procedure), insufficient performance in only one of the test cases. In that case, the parameters converge exceptionally rapidly towards the parameter limits. In the majority of the cases, optimisation designs are obtained that are comparable to the manual work with advantages in constraints, e.g., lower blade loads or few cavitation or cavity shapes associated with a higher margin to cavitation erosion, such as removed mid-chord cavitation.

The purpose of paper VI is also to apply an automated optimisation procedure to a wide range

of test propellers and evaluate the optimal results to determine propeller-dependent optimisation settings. The optimised propellers are, with respect to the applied settings, reasonably good; the designer may, however, consider design limitations that are beyond the applied evaluation methods. However, the generated designs guide the designer to find better solutions faster. To determine reliable guidelines for optimisation settings, further optimisations need to be assessed and categorised according to the propeller design demands, e.g., a focus on cavitation, propeller efficiency or pressure pulse. In that context, the optimisation routine can be improved regarding stricter consideration of the K_T constraint and in complexity, e.g., considering several operating conditions or interchangeable settings of the objectives and constraints can be beneficial to achieve better and possibly novel designs faster.

An expert is a person who has made all the mistakes that can be made in a very narrow field.

Niels Bohr

6 Discussion

The aim of this thesis is to further improve the procedure of propeller design by supplementing the propeller designer with automated optimisation. The approach should assist the designer in finding better designs faster while simultaneously enhancing multi-disciplinary evaluation to reduce the lead time for propeller development and increase the quality of a design. Two tracks are therefore examined, namely, the strategies for optimisation and the improvement of constraints, and both are aligned with the manual design procedure.

In the previous chapter 5, the performed work was outlined and the results of each study were discussed separately. This chapter aims to provide a holistic perspective and show how the research is connected.

In the papers attached to this thesis, the complexity of optimisation is consistently increased to take the optimisation procedure to the same level of design considerations as done by an experienced designer. In this manner, the optimisation outcome becomes more competitive with the manual design and thus more useful for the designer to find new designs faster and with less user interaction.

The work performed for this thesis continues thematically where Han (2008) finished with the optimisation of propeller blade geometry in interaction with the ship hull and the rudder, but with consideration of sheet cavitation as a design constraint. This set-up is the desired approach in propeller design because of the interaction effects between the propeller and its inflow, as well as a direct coupling to the hull geometry. Ideally, the propeller designer has the responsibility of designing the entire propulsion unit, including the hull lines of the aft ship to take interaction effects into account (Grunditz, 2015). Han (2008) also recommends including optimisation of the rudder geometry. However, simultaneously optimising hull lines and the propeller blade geometry enlarges the design space considerably and accordingly requires more evaluations of design alternatives. Numerical effort typically hinders such optimisation. In this thesis, the computational effort of such optimisation with hull interactions is addressed in a set-up of the numerical simulations that consistently considers the computational effort by reducing the mesh size (with consideration of the accuracy) to a *zonal approach*, computing the propeller performance in a hybrid-RANS approach and re-using the converged simulations of the baseline design for the computation of a new variant. However, the numerical effort is considerable and hardly compatible with automated optimisation in a daily routine.

Optimisation algorithms require a certain number of objective function evaluations to gather

knowledge of the problem definition before they can converge to 'the optimal' solution. Throughout this thesis, optimisations are entirely based on population-based optimisation algorithms. This has several reasons: population-based algorithms are to the greatest extent independent from the starting point of the optimisation and are able to find the global optimum, they are independent from continuity of objective functions and objectives, and they are, unlike e.g. adjoint methods, readily applicable in unsteady flow simulations and generally very robust. However, the algorithms require a large number of evaluations, which increase with the number of design variables and constraints.

The lack of convergence is particularly evident from the optimisation performed in paper I, where too many decision variables are applied in combination with a population size that is too small. The optimisation is additionally hindered by numerous constraints that are neither aligned with each other nor with the objective functions. However, the outcome of the optimisation provides awareness of the effect of the blade geometry on the effective wake and, most importantly, a connection between the predicted cavity shape and the pressure pulse objective, as well as the need for improved optimisation methods, from which the emphasis of this thesis originates. In paper I, the assessment of the optimisation outcome provides a relation between the cavity shape and the propeller-induced pressure pulses and indicates a minor impact of cavitation volume on the efficiency. This initiated the first track that is followed throughout this thesis. The cavitation constraints in paper I are applied according to (Han et al., 2006) and refined in terms of cavity shape evaluation and a broadened range of calculated time steps that are interrogated. Han et al. (2006) examined only the angular blade position with the maximum cavity volume, which is reasonable when only the maximum cavity volume is constrained. However, when certain types of cavity shapes have a greater effect on the applied objectives, as indicated in paper I and paper VI, a refined evaluation is important.

Throughout this thesis, cavity shape constraints are refined. From the incipient constraints for the global appearance of cavitation, they evolved to specialised shape constraints with either an explicit effect on the pressure pulse objective, e.g., the change in cavity volume, or an implicit effect on the objectives by reducing, for instance, the thickness of the sheet cavity or by controlling the cavity shape and location on the blade. The latter is also utilised to avoid global cavitation that is known to possibly result in erosive local cavitation, as discussed in paper V and related to Bark et al. (2004) and Foeth (2008). Although they are developed in connection with the prediction of a potential flow simulation prediction, they can readily be transferred to high-fidelity methods.

The evaluation of cavitation constraints for automated optimisation is generally seldom addressed to such a detailed level of cavitation interrogation. In the majority of propeller optimisations, only the general cavitation amount is constrained, if at all. Han et al. (2006) utilises the cavitation volume and sectional cavitation area, pressure coefficient and Keller criteria; Kamarlouei et al. (2014) also applies the Keller criteria as well as the Bucket diagram; Gaggero et al. (2009) and Bertetta et al. (2012) use the cavity plan form area. All apply potential methods for predicting the propeller performance. However, the constraints are rather useful for constraining only the total amount of cavitation rather than the location and shape. A restriction on the cavity shape results in possible trade-off solutions, which allow for higher propeller efficiency. The majority of optimal solutions, obtained from optimisation throughout this thesis, provide a reduction in cavity volume, which is related to the consequent restriction of cavity constraints, relative to the corresponding baseline design.

It is crucial for automated optimisation to present information regarding a design solution in

single values. Gaggero et al. (2009) and Bertetta et al. (2012) apply cavitation as a constraint in propeller efficiency and propeller noise optimisation by averaging different working conditions related to a statistical analysis of the wake field, thereby reducing the information obtained from the flow simulations to a single averaged value. This is adequate for the applied cavitation constraint on the cavity plan form area. However, the aim of an intricate analysis of the sheet cavity formation requires a finer interrogation of the prediction, which is accomplished by the conservative approach of determining the blade position with the maximum cavity volume (*key-blade*) and including the significant blade positions in the vicinity of the key-blade, from which the worst cavity shape constraint is selected.

Evidently, the cavity shape improves with the assistance of the proposed cavity shape constraints. However, the optimal trade-off propeller in paper III frequently provides results that shifted the cavitation towards blade positions that are not assessed during the optimisation. Such behaviour is similarly obtained from the optimal solution of Opt-1 6.1c and the optimal result from paper I (figure 6.1a). The manual design of Opt-1 also yields, however, a shifted cavitation volume towards later blade positions. Such behaviour is certainly beneficial for the pressure pulse objective but can still lead to erosive cavitation outside the interrogated blade positions. This is particularly obvious from Opt-4 6.1f, where only the assessed blade positions achieve a reduction in cavitation volume, although the cavity volume is notably small. Figure 6.1 presents the normalised change cavitation volume (Δ_{maxVol}/R^3), referenced to the baseline design. Thus, if the manually designed benchmark or the optimised solution provide Δ_{maxVol}/R^3 below zero, there is a reduction in volume. For the majority of the cases optimised throughout this thesis, the cavitation is improved and from the comparison in figure 6.1 typically more restrictive regarding cavity volume compared to the benchmark designs. The optimisation outcome still requires critical assessment by an experienced designer to avoid the risk of optimised results that are biased by the tools or constraints applied.

Constraints that are adapted to the objectives increase the connection between the optimisation aim and the decision variables, which improves the behaviour of the optimisation algorithm to enhance convergence and thereby reduce the lead time; this is the second track followed throughout this thesis. The first paper starts with a detailed analysis of the propeller working in the flow field around the hull and indicates that this interaction is important for ensuring a robust design, but in the design phase when exploring the design space, it is impractical due to a long evaluation per variant. Han (2008) already indicated the need for reduced computational time and recommended response surface estimations as a possible remedy.

Consequently, the lead time of propeller optimisation is particularly addressed in paper II, focusing on the ability to substitute computations with estimations by meta-models. The application of meta-models in optimisations as well as optimisation in marine applications is not uncommon, e.g., Schmitz et al. (2002), Maisonneuve (2003) or Harries (2010). However, regarding propeller design, the reported research abates, and most of the recent research is restricted to hydrodynamic force predictions, e.g., (Roddy et al., 2008) and (Calcagni et al., 2010); only Koushan (2000) includes the estimation of propeller-induced pressure pulse by an artificial neural network.

The application of meta-models for propeller optimisation including cavitation constraints is challenging, as indicated by the results from paper II. The performance of meta-models on the propeller performance, predicted by the potential flow simulation, varies both among the meta-models and the quantity that is estimated. In particular, the cavity shape constraints are hardly captured correctly; only the correct trends could be realised. However, optimisation that

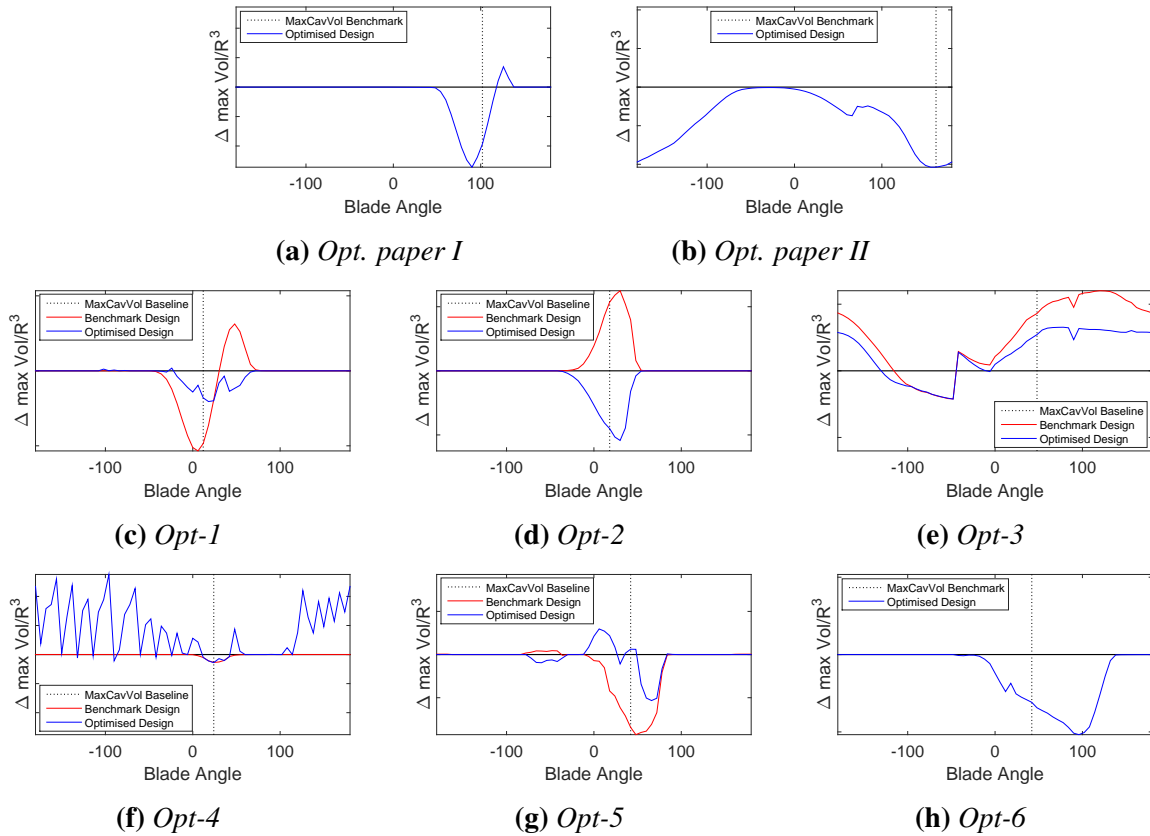


Figure 6.1: Change in cavitation volume per blade angle with respect to baseline designs

is assisted by the Kriging response surface results in a beneficial application, particularly with reduced design space, as indicated in paper VI.

The lead time of propeller optimisation is, however, also addressed in paper IV and paper V with the development of optimisation algorithms and strategies and constraint handling to improve the convergence rate of the optimisation and thus the required number of variant evaluations. The aim of this thesis is to make propeller optimisation more stable, reliable and applicable for everyday use. Consequently, more constraints are required to guide the optimisation to achieve practical designs; this is essentially contradictory to optimisation convergence. Puisa et al. (2011) presents an approach for constraint handling in connection with the NSGA-II algorithm that treats infeasible individuals as single-objective problems with only one objective (the violated constraint); consequently, it converges faster to feasible regions. However, this yields, to a certain extent, a deterioration of the actual objectives. Ray et al. (2009) introduces infeasibility handling to an evolutionary algorithm, which preserves marginally infeasible variants in a population. A violation measure is introduced as an additional objective. However, the violation considers only whether a constraint is violated and not to which extent. The constraint violation measure introduced in paper V attempts to allow for infeasibility within a population if there are other constraints that are superior and that can balance the performance of such variant. In this manner, the manual judgement is imitated and the characteristics of a variant that performs sufficiently regarding one constraint, but insufficiently in the other, are still preserved. Therefore, a violation measure that determines the extent of the violation is required.

An additional approach to improve the convergence is addressed with an importance analysis of decision variables for the optimisation. Paper III presents an extension of the input importance

analysis utilised in paper II, with a sensitivity analysis of input parameters and their importance on propeller characteristics. The employed sensitivity analysis enables a higher order of parameter effects and is applied in similar approaches to reduce the input parameters for prediction methods (e.g., Roos et al., 2012 and Sánchez-Heres et al., 2012). A reduction of input parameters significantly improves the capability of the meta-models, as indicated by the results in paper II and paper VI. However, the types of applied parameters are also important for the quality of the meta-model. Although the performance of the AS NSGA-II is defective, applied together with the parametric geometry curves, the capabilities are enhanced when applying the meta-model together with less localised geometry input parameters.

The input parameter analysis in paper III missed, however, an important parameter: the blade chord length, which typically has a effect on the efficiency. This flaw can be related to either deficient application of the sensitivity analysis or insufficient parameter effects. Because there is no indication from the other parameters that the input samples for the sensitivity analysis are incorrect, it is related to the geometry variation of the chord, which is too small. The application of sensitivity analysis for parameter importance is of avail. However, an explicit analysis, e.g., with the extended FAST method as applied in papers III, V and VI, may not be compulsory. A variance-based sensitivity analysis method can readily be subject to insufficient variances, and predicted parameter influences may be misinterpreted, which yield a premature convergence of a subsequent optimisation. It is, in the author’s view, sufficient to evaluate the generated designs, for instance, created during the outlined primary optimisation, in terms of parameter development. The judgement of an experienced designer is equally valuable.

A general observation from paper VI is that the optimisation yields propeller designs with performance comparable to that of the manually designed propeller. In particular, the optimisation by local curve modifications provide similar geometry trends compared with the benchmark propeller, provided that the correct and effective parameter modifications are selected by the designer. Figures 6.2 to 6.5 provide the parameter changes compared to the baseline design for a subset of parameters of the optimisation in paper VI. The baseline design is represented as the neutral axis. In the majority of the cases, the optimised geometry coincides with the manually designed blade geometry. However, manual modification of skew and chord are more ambitious and even more localised than the changes applied in paper VI.

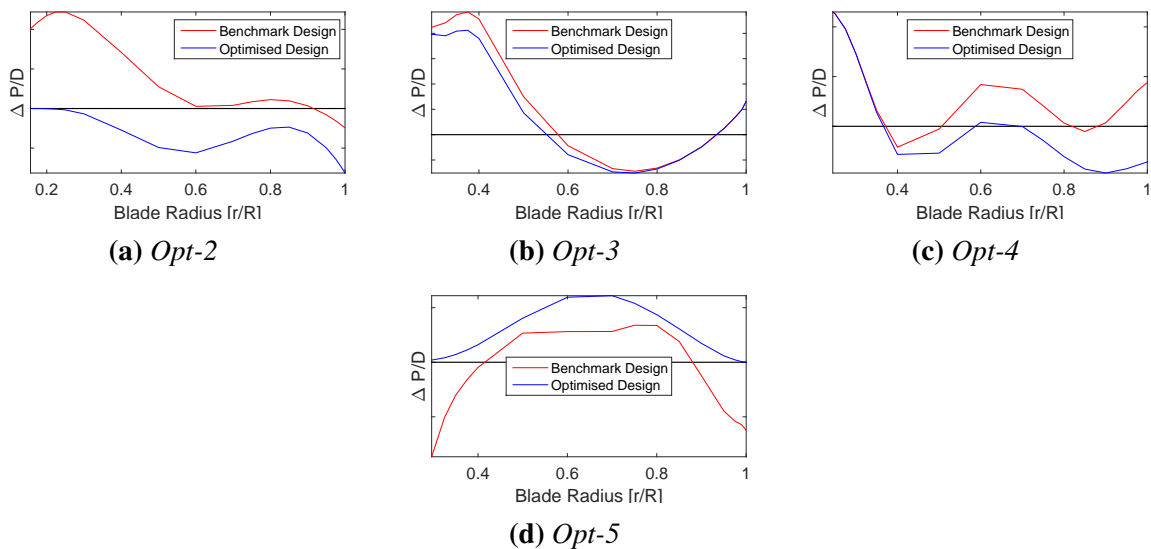


Figure 6.2: Pitch geometry change of benchmark design and optimised design relative to baseline design

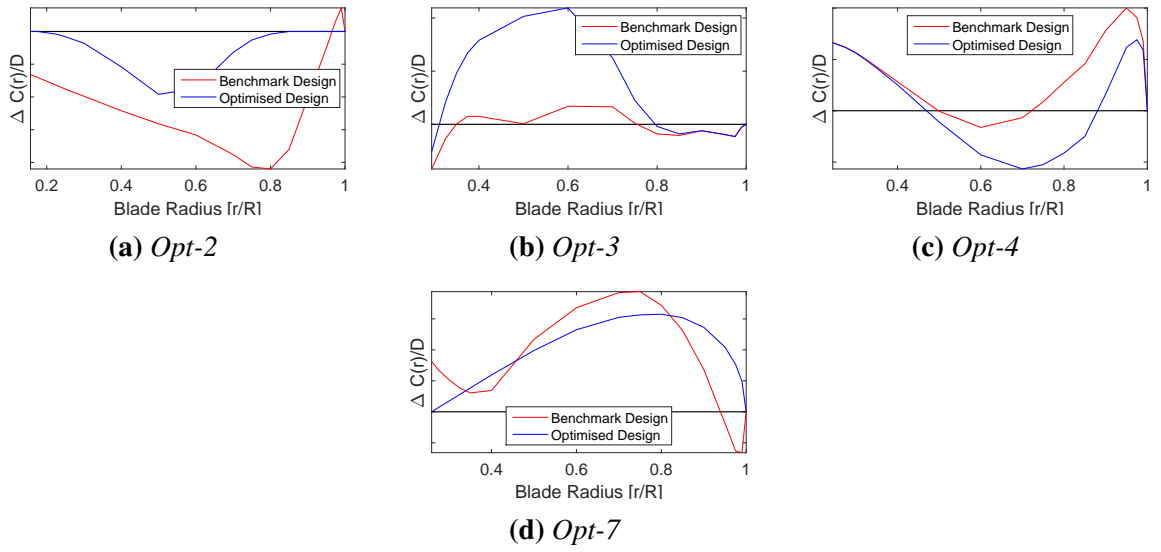


Figure 6.3: Chord geometry change of benchmark design and optimised design relative to baseline design

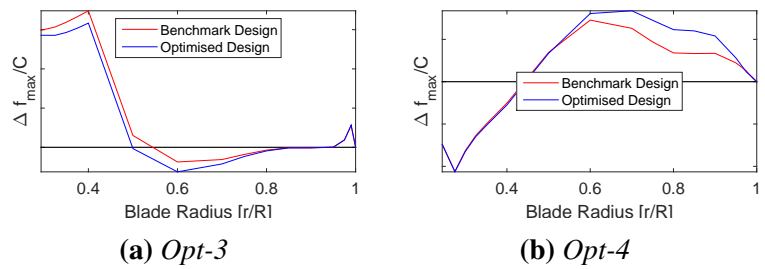


Figure 6.4: Camber geometry change of benchmark design and optimised design relative to baseline design

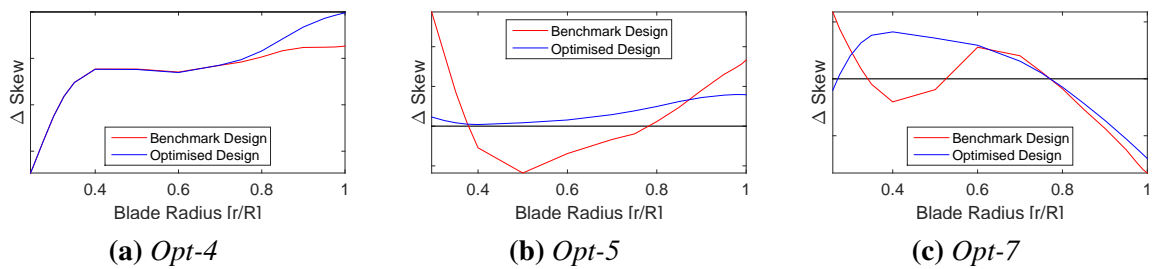


Figure 6.5: Skew geometry change of benchmark design and optimised design relative to baseline design

It is not knowledge, but the act of learning,
not possession but the act of getting there,
which grants the greatest enjoyment.

Carl Friedrich Gauss

7 Conclusion

Propeller design is fascinating. In principle, propellers appear to be interchangeable; the general design has not changed in approximately 100 years. However, each design is unique, and the flow around the propeller blades is remarkably complex, which requires attention in the design of a propulsion unit. The goal of this thesis conforms to this attention by improving the procedure of propeller design through automated optimisation as a supplementary tool to assist the designer in finding better designs faster.

Two tracks are followed to improve automated propeller design: i) the development of strategies and concepts for propeller optimisation, with the objective of developing optimisation algorithms with enhanced convergence and consideration of constraints, and ii) the extension and exploration of constraints that are adapted to the principles and design considerations of the manual design procedure. The work performed on the two tracks contributes to further developing population-based optimisation algorithms and constraints that automatically judge the cavitation on the propeller. Additional constraints and limitations are added to the optimisation procedure, which are often neglected in study cases but that commonly have to be considered by the designers. The algorithms and constraints are implemented in the designer's toolbox for computer-aided propeller design and can be used on an everyday design task with access to all analysis tools available to the designer.

The optimisation procedure handles multi-disciplinary evaluation of multiple objectives and constraints without user interaction; still, it yields propeller designs that are comparable with a manually designed propeller. The developed algorithms are persuasive in their ability to handle constraints, which relates to a memory effect from storing the best solutions in the PSO and a continuous evaluation of the neighbourhood in the SANA NSGA-II. Both algorithms are advantageous in the applied cases compared to the NSGA-II. The AS NSGA-II provides a tremendous benefit in lead time while achieving the same results as the NSGA-II when applied with local curve modification. To determine reliable guidelines for optimisation settings, further optimisations need to be assessed and categorised according to the propeller design demands, e.g., a focus on cavitation, propeller efficiency or pressure pulse. However, the proposed preliminary and supportive optimisation is one step in that direction and enhances the expectation of truly finding an optimal design.

Cavitation constraints clearly improve the quality of the optimisation outcome and the convergence of the optimisation by enhancement of the objective. The pressure pulse objective is

evidently related to certain types of cavitation and frequently provides in the conducted optimisation the largest possible gains, which is related to the focus on cavitation constraints. Thus, in cases with a clear focus on the efficiency, it may be beneficial to consider the pressure pulse as a constraint rather than an objective.

The manual design is superior in terms of design quality, but automated optimisation possesses the advantage of a broader exploration of the design space at the same lead time. There is, however, no evidence that optimisation guarantees better results. Optimisation, manual or automated, is subject to applied limitations provided by, e.g., analysis tools. The manual design is advantageous because the designer may consider limitations that are not provided by any analysis tools. It is still the designer's responsibility to set up a suitable combination of objectives, constraints and decision variables to achieve a successful optimisation. With an improved and faster algorithm, the designer could be able to proceed towards the next design cycle in a shorter amount of time.

The more I learn, the more I realize how much I don't know.

Albert Einstein

8 Further Work

The development of innovative optimisation algorithms and strategies suited for propeller design optimisation will not end here. Automated optimisation for practical applications is just emerging. The general question is what to prioritise: the accuracy or the usability. Computational methods of higher fidelity analysis are typically more accurate and provide more details on the flow around the propeller blade because they comprise more physical reality than potential methods. However, the practical application of optimisation methods requires the consideration of numerous limitations, which can easily be extended from those realised within this thesis. Consequently, the most obvious improvement can be realised with variable fidelity optimisation, composed of RANS simulations, potential flow simulations and meta-models, together with an algorithm that is able to decide which evaluation to utilise. However, the optimisation with consideration of the hull is still too demanding in the general blade geometry finding phase.

Further work, despite the fidelity of numerical evaluation methods, can be categorised into *optimisation and propeller design*, *constraints development* and *optimisation guidance*.

Optimisation and propeller design

The optimisation algorithms should be further developed to automatically resolve when to analyse the propeller with simulations and when meta-model estimations are sufficient. The decision will thus depend on both the current training status of the meta-model and the distance of the parameter location in the design space relative to other computed solutions. Such a decision routine can readily be extended to several levels of variable fidelity, but with careful consideration of matching constraints and objective representation of the different analysis tools.

Automated optimisation has the potential to become superior to manual design. The presented optimisation outlines a routine that imitates the manual design process to assist the designer. However, the optimisation can readily be extended to additionally consider several off-design conditions simultaneously and thereby enhance the product quality by adaptation to the entire life cycle of the propeller and not only a single design point. In the case of a CPP, this will include an underlying optimisation of the optimal blade pitch adjustment for the off-design conditions. Manual design is of course capable of such optimisation; however, lead time typically restricts such extensive investigations.

Introducing several conditions to the optimisation can also be used for optimisation in a semi-unsteady wake, e.g., to account for the changing inflow to the propeller in waves. In such a scenario, the efficiency could be considered as an aggregated function, while the constraints are subject to the most deficient performance.

Constraints

Automated optimisation depends more on the specified limitations and capabilities of the applied analysis tools than manual design. Several considerations of the designer during the manual design process can be considered by the parameter limits, e.g., maximum rake to avoid interference with the hull or pod. However, there are important design considerations that have to be considered during the optimisation by simulations, e.g., tip vortex inception. Consequently, the continuous development of analysis tools is part of future work for propeller optimisation to further improve possible constraints. Hence, we are improving a semi-analytical method for tip vortex inception based on the simulations of a vortex lattice potential flow simulation. New cavitation constraints are also under development for indicating erosive cavitation by evaluation of the cavitation collapse.

However, the proposed constraints on cavitation could also be improved to be more flexible and adaptable to the cavitation on the baseline design. Particularly, the cavitation closure line harm-factor performed disappointingly due to lacking similarity between the specified polynomial and the simulated cavitation shape. This will be cured by fitting the polynomial to the cavity shape of the baseline. However, other potential methods that are able to indicate the re-entrant jet are interesting to be included in the optimisation and constraints development.

Optimisation guidance

Eventually, the strategies for automated propeller optimisation will become more diverse yet useful in particular problems. Hence, it is recommended to establish a database for optimisation problems with respect to propeller design demands, e.g., a focus on cavitation, propeller efficiency or pressure pulse. This should lead to the determination of reliable guidelines for optimisation settings.

References

- Abdel-Maksoud, M., ed. (2011). *Proceedings of the Second International Symposium on Marine Propulsors*. (Hamburg, Germany). Hamburg University of Technology.
- Andersen, P., A.-S. Borrod, and H. Blanchot (2005). Evaluation of the service performance of ships. *Marine Technology* **42.4**, 177–183.
- Backlund, P. B., D. Shahan, and C. C. Seepersad (2010). Metamodeling techniques for multidimensional ship design problems. *Ship Science & Technology* **4.7**, 43–54.
- Bark, G., N. Berchiche, and M. Grekula (2004). *Application of principles for observation and analysis of eroding cavitation - The EROCAV observation handbook*. Report. Dept. of Naval Architecture and Ocean Engineering.
- Benini, E. (2003). Multiobjective design optimization of B-screw series propellers using evolutionary algorithms. *Marine Technology* **40.4**, 229–238.
- Berger, S. et al. (2014). A Two-Stage Optimisation Method for Full-Scale Marine Propellers Working Behind a Ship. *Ship Technology Research* **61.2**, 64–79.
- Bertetta, D. et al. (2012). CPP propeller cavitation and noise optimization at different pitches with panel code and validation by cavitation tunnel measurements. *Ocean Engineering* **53**, 177–195.
- Bertram, V. (2012). *Practical ship hydrodynamics*. Elsevier.
- Binns, J., R. Brown, and N. Bose, eds. (2013). *Proceedings of the Third International Symposium on Marine Propulsors*. (Launceston, Tasmania, Australia). University of Tasmania.
- Blount, D. (1993). “Prospects for Hard Chine, Monohull Vessels”. *Proceedings: FAST’93*.
- Box, G. E. and K. Wilson (1951). On the experimental attainment of optimum conditions. *Journal of the Royal Statistical Society. Series B (Methodological)* **13.1**, 1–45.
- Breslin, J. P. et al. (1982). Theoretical and experimental propeller-induced hull pressures arising from intermittent blade cavitation, loading, and thickness. *Transactions-Society of Naval Architects and Marine Engineers* **90**, 111–151.
- Burnside, O. H., D. D. Kana, and F. E. Reed (1979). A design procedure for minimizing propeller induced vibration in hull structural elements. Export Date: 17 July 2012 Source: Scopus.
- Calcagni, D. et al. (2010). “Automated Marine Propeller Design Combining Hydrodynamics Models and Neural Networks”. *First International Symposium on Fishing Vessel Energy Efficiency E-Fishing*.
- Carlton, J. (2007). “22 - Propeller design”. *Marine Propellers and Propulsion (Second Edition)*. Ed. by J. Carlton. Second Edition. Oxford: Butterworth-Heinemann, pp. 435–463.
- Chandrashekarappa, P. and R. Duvigneau (2007). *Radial basis functions and kriging metamodels for aerodynamic optimization*. Tech. rep. 6151. Unité de recherche INRIA Sophia Antipolis.
- Costa, J., L. Pronzato, and E. Thierry (1999). “A comparison between Kriging and radial basis function networks for nonlinear prediction.” *NSIP*, 726–730.
- Cummings, D. E. (1973). Numerical Prediction of Propeller Characteristics. *Journal of Ship Research* **17.1**. cited By 0, 12–18.
- Deb, K. and R. B. Agrawal (1995). Simulated Binary Crossover for Continuous Search Space. *Complex Systems* **9**, 115–148.
- Deb, K. and M. Goyal (1996). A Combined Genetic Adaptive Search (GenaAS) for Engineering Design. *Computer Science and Informatics* **26**, 30–45.
- Deb, K. et al. (2002). A Fast Elitist Multi-Objective Genetic Algorithm: NSGA-II. *IEEE Transactions on Evolutionary Computation* **6**, 182–197.
- DNV (2010). *Rules for Classification of Ships*. Det Norske Veritas.
- (2012). *Calcualtion of Marine Propellers*. Det Norske Veritas.

- Ellbrant, L. (2014). *Multi-objective CFD-based design method for axial compressors*. Chalmers University of Technology.
- Fine, N. E. (1992). “Nonlinear Analysis of Cavitating Propellers in Nonuniform Flow”. PhD thesis. Massachusetts Institute of Technology.
- Foeth, E.-J. (2008). “The structure of three-dimensional sheet cavitation”. PhD Thesis. University Delft.
- (2015). “Propeller optimization using an unsteady Boundary-Element Method”. *Fourth International Symposium on Marine Propulsors*. Ed. by S. A. Kinnas. Vol. II. The University of Texas at Austin, 27–32.
- Froude, R. (1889). On the part played in propulsion by differences of fluid pressure. *Transactions of the Institute of Naval Architects* **30**, 390–405.
- Gaggero, S and S Brizzolara (2009). “Parametric CFD optimization of fast marine propellers”. *10th International Conference on Fast Sea Transportation, Athens, Greece*.
- Goldstein, S. (1929). On the Vortex Theory of Screw Propellers. *Proceedings of the Royal Society of London A: Mathematical, Physical and Engineering Sciences* **123**.792, 440–465.
- Greeley, D. S. and J. E. Kerwin (1982). Numerical methods for propeller design and analysis in steady flow. *Transactions-Society of Naval Architects and Marine Engineers* **90**, 415–453.
- Griffin, P (1998). “Computational techniques for the design and analysis of cavitating propeller blades”. Master’s thesis.
- Griffin, P. E. and S. A. Kinnas (1998). A Design Method for High-Speed Propulsor Blades. *Journal of Fluids Engineering* **120**.3, 556–562.
- Grunditz, G. (2015). Optimizing Propeller and Propulsion. *Marine Technology* **52**.1, 48–55.
- Han, K.-J. (2008). *Numerical optimization of hull/propeller/rudder configurations*. [Doktorsavhandlingar vid Chalmers tekniska högskola]. Ny serie, Göteborg: Chalmers University of Technology, xii, 88 s.
- Han, K.-J., G. Bark, and B. Regnstrom (2006). A Procedure for Optimizing Cavitating Propeller Blades in a Given Wake. *Ship Technology Research* **53**.1, 39–52.
- Harries, S. (2010). “Investigating Multi-dimensional Design Spaces Using First Principle Methods”. *Seventh International Conference On High-Performance Marine Vehicles (HIPER)*.
- He, L (2010). “Numerical simulation of unsteady rotor/stator interaction and application to propeller/rudder combination (UT-OE Report 10-05)”. PhD thesis. University of Texas at Austin, Dept. of Civil Engineering.
- He, L., S. Chang, and S. Kinnas (2010). *MPUF-3A Version 3.0*. Report. University of Texas.
- He, L., Y. Tian, and S. Kinnas (2011). *MPUF-3A Version 3.1*. Report. University of Texas.
- Hildebrand, J. A. (2009). Anthropogenic and natural sources of ambient noise in the ocean. *Marine Ecology Progress Series* **395**, 5–20.
- ISSC, ed. (2006). *Dynamic Response*. Vol. 1. 16th International Ship and Offshore Structures Congress.
- ITTC (1999). *ITTC – Recommended Procedures; Performance, Propulsion 1978 ITTC Performance Prediction Method*. International Towing Tank Conference.
- (2002). “The Specialist Committee on Speed and Powering Trails”. 2. ITTC. 23rd International Towing Tank Conference.
- (2008). *ITTC – Recommended Procedures and Guidelines; Testing and Extrapolation Methods, Propulsion, Performance, Predicting Powering Margins*. International Towing Tank Conference.
- Janson, C and L Larsson (1996). “A method for the optimization of ship hulls from a resistance point of view”. *21st Symposium on Naval Hydrodynamics, Trondheim, Norway*.
- Kamarlouei, M. et al. (2014). Multi-objective evolutionary optimization technique applied to propeller design. *Acta Polytechnica Hungarica* **11**.9, 163–182.

- Kerwin, J, S Kinnas, and M. Wilson (1986). “Experimental and analytical techniques for the study of unsteady propeller sheet cavitation”. *Symposium on Naval Hydrodynamics, 16th*. Ed. by W. C. Webster. Office of Naval Research, National Academy Press, 387–414.
- Kerwin, J. E. (1961). “The solution of propeller lifting surface problems by vortex lattice methods”. PhD thesis. DTIC Document.
- Kerwin, J. E. and J. B. Hadler (2010). Principles of Naval Architecture Series: Propulsion. *The Society of Naval Architects and Marine Engineers (SNAME)*.
- Kinnas, S. and N. Fine (1989). “Theoretical prediction of midchord and face unsteady propeller sheet cavitation”. *International Conference on Numerical Ship Hydrodynamics, 5th*.
- Kinnas, S. A. (1985). “Non-Linear Corrections to the Linear Theory for the Prediction of the Cavitating Flow Around Hydrofoils.” PhD thesis. Massachusetts Institute of Technology.
- Kinnas, S. A. (1991). Leading-edge corrections to the linear theory of partially cavitating hydrofoils. *Journal of Ship Research* **35.1**, 15–27.
- (1996). An international consortium on high-speed propulsion. *Marine Technology and SNAME News* **33**, 203–210.
- Kinnas, S. A. and N. E. Fine (1993a). A numerical nonlinear analysis of the flow around two-and three-dimensional partially cavitating hydrofoils. *Journal of Fluid Mechanics* **254**, 151–181.
- (1993b). A numerical nonlinear analysis of the flow around two-and three-dimensional partially cavitating hydrofoils. *Journal of Fluid Mechanics* **254**, 151–181.
- Koushan, K. (2000). “Prediction of Propeller Induced Pressure Pulses Using Artificial Neural Networks”. *1st International Conference on Computer Application and Information Technology in Maritime Industries*, 248–254.
- Kutta, W. (1910). Über eine mit den Grundlagen des Flugproblems in Beziehung stehende zweidimensionale Strömung. Sitzungsbericht d. *Bayr. Akad. d. Wiss., math.-phys. Klasse, München* **2**, 65.
- Lee, C.-S. (1979). “Prediction of steady and unsteady performance of marine propellers with or without cavitation by numerical lifting-surface theory”. PhD thesis. Massachusetts institute of Technology.
- Lee, C.-S. et al. (2010). Performance optimization of marine propellers. *International Journal of Naval Architecture and Ocean Engineering* **2.4**, 211–216.
- Lee, S.-K., M. Liao, and S. Wang (2006). “Propeller-induced hull vibration—analytical methods”. *Proceedings of the second international ship noise and vibration conference. London, UK, June*. Vol. 28. Citeseer.
- Lerbs, H. W. (1952). Moderately loaded propellers with a finite number of blades and an arbitrary distribution of circulation. *Trans. SNAME* **60**.
- Maisonneuve, J.-J. (2003). “Application Examples From Industry”. *OPTIMISTIC Optimization in Marine Design*. Ed. by L. Birk and S. Harries. Berlin: Mensch & Buch Verlag. Chap. 7, pp. 151–172.
- MAN (2011). *Basic Principles of Ship Propulsion*.
- Mishima, S. (1996). “Design of Cavitating Propeller Blades in Non-Uniform Flow by Numerical Optimization”. PhD Thesis. Massachusetts Institute of Technology.
- Munk, M. M. (1919). *Isoperimetrische Aufgaben aus der Theorie des Fluges*. Göttingen: Dieterichsche Universitäts-Buchdruckerei.
- Olsen, S. A. (2001). “Optimisation of propellers using the vortex-lattice method”. PhD thesis. Technical University of Denmark.
- Peri, D. (2009). Self-Learning Metamodels for Optimization. *Ship Technology Research* **56.3**, 95–109.
- Prandtl, L and A Betz (1919). Schraubenpropeller mit geringstem Energieverlust. *Göttinger Nachrichten* **2**.

- Prandtl, L. (1918). Tragflügeltheorie. I. Mitteilung. *Nachrichten von der Gesellschaft der Wissenschaften zu Göttingen, Mathematisch-Physikalische Klasse* **1918**, 451–477.
- Puisa, R. and H. Streckwall (2011). Prudent constraint-handling technique for multiobjective propeller optimisation. English. *Optimization and Engineering* **12.4**, 657–680.
- Rankine, W. J. M. (1865). *On the mechanical principles of the action of propellers*. publisher not identified.
- Ray, T. et al. (2009). “Infeasibility Driven Evolutionary Algorithm for Constrained Optimization”. *Constraint-Handling in Evolutionary Optimization*. Ed. by E. Mezura-Montes. Vol. 198. Studies in Computational Intelligence. Springer Berlin Heidelberg. Chap. 7, pp. 145–165.
- Regnström, B. (2007). *XCHAP theoretical manual*. Flowtech International AB, Gothenburg.
- Roddy, R. F., D. E. Hess, and W. Faller (2008). “Utilizing neural networks to predict forces and moments on a submarine propeller”. *46th AIAA Aerospace Sciences Meeting and Exhibit*.
- Roos, D., K. Cremans, and T. Jasper (2012). “Probability and variance-based stochastic design optimization of a radial compressor concerning fluid-structure interaction”. *9th Weimar Optimization and Stochastic Days*.
- Sánchez-Heres, L. F., J. W. Ringsberg, and E. Johnson (2012). Study on the possibility of increasing the maximum allowed stresses in fiber-reinforced plastics. *Composite Materials* **47.16**, 1931–1941.
- Sasaki, D., S. Obayashi, and H.-J. Kim (2001). “Evolutionary algorithm vs. adjoint method applied to sst shape optimization”. *The Annual Conference of CFD Society of Canada, Waterloo*.
- Schmitz, A., E. Besnard, and E. Vives (2002). “Reducing the cost of computational fluid dynamics optimization using multi layer perceptrons”. *Proceedings of the International Joint Conference on Neural Networks*. Vol. 2, 1877–1882.
- Smith, T. et al. (2014). Third IMO GHG Study 2014. *International Maritime Organization (IMO), London*.
- Sun, H. and S. Kinnas (2007). *HULLFPP, HULL Field Point Potential*. Report. University of Texas.
- Tachmindji, A. and W. Morgan (1957). *The design and performance of supercavitating propellers*. Tech. rep. No. DTMB-C-807. DTIC Document.
- Triantafyllou, M. S. (1979). COMPUTER AIDED PROPELLER PRELIMINARY DESIGN USING THE B-SERIES. *Marine Technology Society Journal* **16.4**.
- Tsakonas, S, J Breslin, and M Miller (1967). Correlation and application of an unsteady flow theory for propeller forces. *SNAME Transactions* **75**, 158–193.
- Van Lammeren, W., J. Van Manen, and M. Oosterveld (1969). The Wageningen B-screw series. *Trans. SNAME* **77**, 269–317.
- Van Manen, J. D. (1966). The choice of propeller. *Marine Technology* **3**.
- Van Wijngaarden, H. C. J. (2011). “Prediction of propeller-induced hull-pressure fluctuations”. PhD thesis. Delft University of Technology.
- Vanderplaats, G. N. (2001). *Numerical optimization techniques for engineering design, Vanderplaats Research & Development*. 3rd ed. Vabderplaats Research & Development, Inc.
- Vesting, F. (2010). *Validation of Mpuf-3A v3.0 - Comparison of results from Mpuf-3A v2.3 and v3.0 for 4 different test cases*. Tech. rep. R-674. Rolls-Royce Hydrodynamic Research Centre.
- Vesting, F., R. Gustafsson, and R. Bensow. Development and Application of Optimisation Algorithms for Propeller design. Manuscript submitted for publication to STR Journal of Ship Technology Research.
- Vesting, F. and R. Bensow. Particle Swarm Optimisation: An Alternative in Marine Propeller Optimisation? Manuscript submitted for publication to OPTE Journal of Optimization and Engineering.

- Vesting, F. et al. Procedure for application-oriented Optimisation of Marine Propellers. Manuscript to be submitted for publication to OE Journal of Ocean Engineering.
- Vesting, F. and R. Bensow (2011). “Propeller Optimisation Considering Sheet Cavitation and Hull Interaction”. *Proceedings of the Second International Symposium on Marine Propulsors*. (Hamburg, Germany). Ed. by M. Abdel-Maksoud. Hamburg University of Technology, 79–88.
- Vesting, F., R. Johansson, and R. Bensow (2013). “Parameter Influence Analysis in Propeller Optimisation”. *Proceedings of the Third International Symposium on Marine Propulsors*. (Launceston, Tasmania, Australia). Ed. by J. Binns, R. Brown, and N. Bose. University of Tasmania, 397–404.
- Vesting, F. and R. E. Bensow (2014). On surrogate methods in propeller optimisation. *Ocean Engineering* **88**.0, 214–227.
- Visonneau, M. (2010). “Analysis of G2010 results for test cases 1.1a, 2.1, 2.3a, 3.1a, 3.1b, 3.5 and 3.6 Local flow analysis”. *Gothenburg 2010 Workshop on Numerical Ship Hydrodynamics*. Chalmers University of Technology.
- Vrijdag, A., J. de Jong, and H. von Nuland (2013). “Uncertainty in Bollard Pull Prediction”. *Third Symposium on Marine Propulsors*. Ed. by J. Binns, R. Brown, and N. Bose. Vol. 1, 447–453.
- Young, Y. and S. Kinnas (1999). “Numerical and experimental validation of a cavitating propeller bem code”. *Cavitation and Multiphase Flow Forum*.
- Zou, L. and L. Larsson (2010). “CFD prediction of the local flow around the KVLCC2 tanker in fixed conditions”. *Gothenburg 2010 Workshop on Numerical Ship Hydrodynamics*. Chalmers University of Technology.

